2014

NANOFILTRATION MEMBRANES FROM ORIENTED MESOPOROUS SILICA THIN FILMS

Mary K. Wooten
University of Kentucky, Kaitlyn.wooten@gmail.com

STUDENT AGREEMENT:

I represent that my thesis or dissertation and abstract are my original work. Proper attribution has been given to all outside sources. I understand that I am solely responsible for obtaining any needed copyright permissions. I have obtained needed written permission statement(s) from the owner(s) of each third-party copyrighted matter to be included in my work, allowing electronic distribution (if such use is not permitted by the fair use doctrine) which will be submitted to UKnowledge as Additional File.

I hereby grant to The University of Kentucky and its agents the irrevocable, non-exclusive, and royalty-free license to archive and make accessible my work in whole or in part in all forms of media, now or hereafter known. I agree that the document mentioned above may be made available immediately for worldwide access unless an embargo applies.

I retain all other ownership rights to the copyright of my work. I also retain the right to use in future works (such as articles or books) all or part of my work. I understand that I am free to register the copyright to my work.

REVIEW, APPROVAL AND ACCEPTANCE

The document mentioned above has been reviewed and accepted by the student's advisor, on behalf of the advisory committee, and by the Director of Graduate Studies (DGS), on behalf of the program; we verify that this is the final, approved version of the student's thesis including all changes required by the advisory committee. The undersigned agree to abide by the statements above.

Mary K. Wooten, Student

Dr. Barbara L. Knutson, Major Professor

Dr. Thomas Dziubla, Director of Graduate Studies

NANOFILTRATION MEMBRANES FROM ORIENTED MESOPOROUS SILICA THIN FILMS

THESIS

A thesis submitted in partial fulfillment of the requirements for the degree of Master of Science in Chemical Engineering in the College of Engineering at the University of Kentucky

By

Mary Kaitlyn Clark Wooten

Lexington, Kentucky

Director: Dr. Barbara L. Knutson, Professor of Chemical and Materials Engineering

Lexington, Kentucky

2014

ABSTRACT OF THESIS

NANOFILTRATION MEMBRANES FROM ORIENTED MESOPOROUS SILICA THIN FILMS

The synthesis of mesoporous silica thin films using surfactant templating typically leads an inaccessible pore orientation, making these films not suitable for membrane applications. Recent advances in thin film synthesis provide for the alignment of hexagonal pores in a direction orthogonal to surface when templated on chemically neutral surfaces. In this work, orthogonal thin film silica membranes are synthesized on alumina supports using block copolymer poly(ethylene glycol)-block-poly(propylene glycol)-block-poly(ethylene glycol) (P123) as the template. The orthogonal pore structure is achieved by sandwiching membranes between two chemically neutral surfaces, resulting in 90 nm thick films. Solvent flux of ethanol through the membrane demonstrates pore accessibility and suggests a silica pore size of approximately 10 nm. The permeability of ions and fluorescently tagged solutes (ranging from 4,000 to 70,000 Da) is used to demonstrate the membrane's size selectivity characteristics. A size cut off occurs at 69,000 Da for the model protein BSA. By functionalizing the silica surface with a long chained alkyl group using n-decyltriethoxysilane (D-TEOS), the transport properties of the membranes can be altered. Contact angle measurements and FTIR results show the surface to be very hydrophobic after functionalization. Solvent flux of ethanol through the silica thin film membrane is similar before and after functionalization, but water flux decreases. Thin film silica membranes show much promise for applications in catalysis, bio-sensing, and affinity separations.

KEYWORDS: thin film silica, surfactant templating, mesoporous silica, orthogonal pores, functionalized silica

Mary Kaitlyn Clark Wooten

March 26, 2014

NANOFILTRATION MEMBRANES FROM ORIENTED MESOPOROUS SILICA THIN FILMS

By

Mary Kaitlyn Clark Wooten

Dr. Barbara Knutson
Director of Thesis

Dr. Thomas Dziubla
Director of Graduate Studies

March 26, 2014
Date

TABLE OF CONTENTS

LIST OF TABLES

LIST OF FIGURES

Chapter One: BACKGROUND AND INTRODUCTION
INTRODUCTION

Metal oxide membranes synthesized by sol gel templating have the potential to be versatile platforms for separations on the basis of the ability to control the pore size through templating and synthesis variables, the range of available approaches to functionalize the pores, and the stability of the membranes in the presence of different chemical and biological environments. Surfactant templating of mesoporous thin film silica typically leads to parallel pore alignment with respect to the surface, and therefore inaccessible pores in the potential membrane structure. Recent advances in silica thin film synthesis provide for perpendicular pore alignment by casting on a chemically neutral surface. By providing a chemically neutral surface (Konganti, 2006) for the micelles in the deposited film precursor solution, there will be no preferential affinity for the surfactant micelles to align parallel and it may align perpendicular to the support instead. This method of silica thin film synthesis with accessible pores has the potential to be translated onto a variety of substrates.

By casting the thin silica films on traditional membrane supports, such as anodized alumina oxide (AAO) membranes, silica thin films can be translated into operational membranes with a size selectivity corresponding to their pore size. By depositing a chemically neutral layer of cross linked polymer on the AAO support and then dip coating the silica film on the support, an accessible mesoporous film may be achieved.

The hypothesis of this research is that size and chemically selective separations may be accomplished by the small, uniform hexagonally close packed pore array (hexaganol pores typically in the range of 3 to 10 nm) of the templated silica thin films. The overall goal of this research is to evaluate the membrane properties of thin silica films deposited onto anodized alumina supports that were coated with a chemically neutral surface. The specific objectives of this research were to:

1) Demonstrate the size selectivity separation of the thin film silica membranes using a series of fluorescently tagged molecules (5(6)-carboxyfluorescein and Fluorescein Isothiocyanate (FITC) tagged dextrans ranging from 400 to 70,000 Da). Quantitatively compare the diffusion of solutes in the thin film silica membranes to bare anodized alumina support.
2) Functionalize the thin film membranes with hydrophobic groups to change the properties of the surface. Compare the flux of solvents through functionalized membranes.

BACKGROUND: LOW ENERGY SEPARATIONS

Development of aqueous-based separation technologies for energy, health, and environmental applications relies heavily on low-energy intensive separation alternatives, such as membranes and adsorbents. Membranes and adsorbents use natural processes of diffusion and chemical selectivity to separate substances based on their structure, chemical affinity, or other properties such as hydrophobicity in an energy efficient manner. The membranes are inherently designed to differentiate between chemical or structural difference of the solutes in solution. Applications of such systems include cleaning waste water, separating soluble sugars out of solutions, and even in drug recovery.

Membranes come in two typical varieties, porous and nonporous. Porous membranes have channels throughout their surface which a solute may travel (Figure 1.1 A). The only area of the surface of these membranes that is permeable is that which is void, which corresponds to a specific porosity or void fraction. Nonporous membranes typically involve a chemical specificity to what can permeate; such an example would be a polymeric membrane. Nonporous polymeric membranes are associated with the separation of gases, but have also been demonstrated for the separation of solvents (Darvishmanesh, Degreve, & Van der Bruggen, 2009). These membranes lack pores but the entire surface has the capacity to allow certain molecules to permeate (Figure 1.1 B). Each type of membrane has its specific uses; porous membranes are of interest in this study.

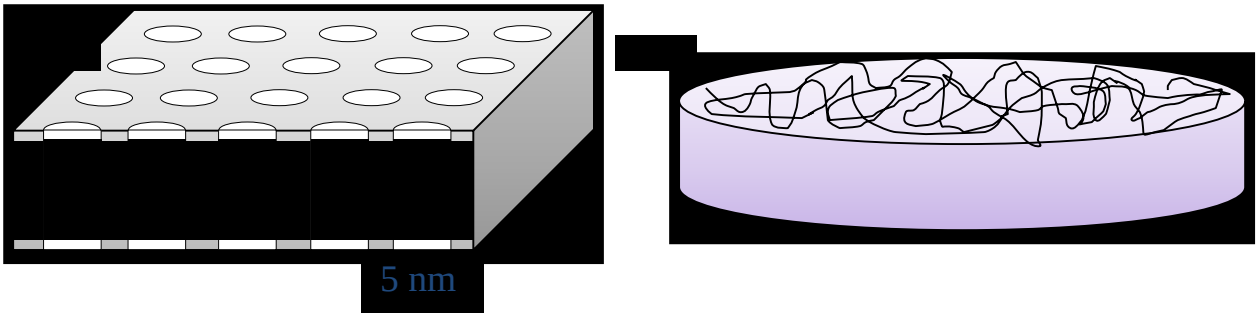

FIGURE 1.1. Membranes a) mesoporous, b) nonporous membrane.

The pore size of porous membranes can range from hundreds of microns to a sub nanometer scale. Table 1 summarizes the different types of filtration that corresponds to specific pore sizes or particles filtered. Larger pores have the ability to remove bacteria and even some viruses while smaller pores can separate sugars and even certain anions or cations. The driving force behind the separation changes based on the separation process such as an electrical potential gradient opposed to a concentration gradient.

Table 1.1. Filtration specifications corresponding to pore sizes of membranes and their separation capabilities. Adapted from Membrane Handbook (*Membrane Handbook*, 2001).

Separation Process	**Nature of Species Retained (size)**	**Nature of Species Transported through Membrane**	**Mechanism for Transport/Selectivity**	**Driving Force**
Gas Permeation	Larger species retained unless highly soluble	Gaseous, Smaller species/ more soluble species	Solution-diffusion in gas	Concentration gradient (partial pressure difference)
Pervaporation	Same as above	More soluble/ smaller/ more volatile nonelectrolytes	Solution-diffusion in liquid free with gaseous permeate	Concentration gradient, temperature difference
Dialysis	>0.2 μm retained, >0.005 μm retained in hemodialysis	Microsolute, smaller solute	Sieving, hindered diffusion in microporous membranes in liquid	Concentration gradient
Electrodialysis	Co-ions, macroions and water retained	Microionic species	Counter-ion transport via ion exchange membranes in liquid	Electrical potential gradient, electro-osmosis
Reverse Osmosis	1 to 10 Å micro-solute species	Solvent, Species retained may be electrolytic or volatile	Preferential sorption/capillary flow in liquid	Hydrostatic pressure gradient vs. osmotic pressure gradient
Ultrafiltration	10 to 200 Å macrosolute species	Solution of microsolutes	Sieving in liquid	Hydrostatic pressure gradient vs. osmotic pressure gradient
Microfiltration	0.02 to 10 μm particles	Solution/gas free of particles	Sieving in liquid or gas	Hydrostatic pressure gradient
Emulsion liquid membrane	Generally not size-selective except in host-guest chemistry	Species with high solubility in liquid membranes	Solution-diffusion, facilitated transport, generally in liquid feed, emulsion containing permeate	Concentration gradient, pH gradient

Mesoporous membranes for ultrafiltration are of particular interest because of their small pore sizes ranging from 2-50 nm in diameter (Davis, 2002)(Figure 1.1). This small pore size leads to a large increase in surface area compared to a non-porous or even macroporous surface. Pores on the nanoscale can lead to a very precise separation based on size seen by the specific gas diffusion coefficients following a Knudsen-type mechanism using mesoporous silica deposited onto an α-alumina support (Boffa, ten Elshof, & Blank, 2007). Coupled with chemical properties, the mesoporous films can achieve very valuable separations or detections such as the detection of benzene and ethanol vapors by mesoporous silica functionalized with beta-cyclodextrin (Palaniappan, Li, Tay, Li, & Su, 2006).

Porous membranes are currently being used as low energy methods of biomass conversion to bio-based chemicals and fuels. By utilizing the small pores, enzymes may be immobilized on the surface to allow products to filter though the pores eliminating product accumulation which can result in lower activities in the enzymes (Ansari & Husain, 2012; Asuri et al., 2007; Cang-Rong & Pastorin, 2009). Such membranes or films have also been studied for methods of drug, particle, and waste detection. The porous support can provide heightened surface area for a more accurate detection method by functionalizing or absorbing chemicals to the surface that detect the specific molecule (Coll, Martinez-Manez, Marcos, Sancenon, & Soto, 2007; Collinson, 1999; Nazeeruddin, Di Censo, Humphry-Baker, & Gratzel, 2006; Palaniappan et al., 2006).

SILICA MATERIALS: SOL-GEL CHEMISTRY

Porous silica has long since been studied because of its thermal and chemical stability in a range of environments (Davis, 2002). It can withstand high temperatures and a range of low pH values but also has the ability for its surface to be functionalized. These materials are typically synthesized using a sol-gel method. The process involves individual monomers being converted into a colloidal system (sol) which then can be integrated into a network (gel) of individual particles or a complex of polymers. This involves the hydrolysis and polycondensation of alkoxide precursors, either acid or base driven, followed by drying and aging of the structure to result in films, particles, or monoliths (Hench & West, 1990). This procedure synthesizes microporous or mesoporous disordered structures.

The use of surfactant templates has also played a role in furthering the field of sol-gel synthesis. Surfactant pore templating involves the use of a micelle template to occupy the space that will eventually be a pore while the alkoxide precursor condenses around the micelle. The removal of the template leads to an empty, accessible pore array. With surfactant templates as pore forming agents, a finer tuning of pores can be achieved through the selection of a template (surfactant or polymer) that forms the desired pore size and structure (Zhao, Huo, Feng, Chmelka, & Stucky, 1998). The resulting pores are within the classification range of mesoporous and therefore can be applied to small solute separations as well. Zhao, et al. obtained SBA-15 particles with hexagonal pore sizes ranging from 50-300 angstroms by varying the reaction temperature and block copolymer template, demonstrating that the pore structures are related to the choice of template and the concentration of template (D. Y. Zhao, J. L. Feng, et al., 1998).

The template and template concentration can be used to obtain different surfactant mesophases that are captured in the final silica structure. A hexagonally closed packed (HCP), cubic, or worm like structure (Figure 1.2) can be achieved, each with its own advantages and disadvantages (Alberius et al., 2002; Lu et al., 1997). Pores through thin films have the ability to be aligned parallel or perpendicular to the substrate they are deposited on depending on the application of the film. Cubic and worm-like pores are structurally 3D making them accessible but interconnected leading to high tortuosity and potentially limited mass transfer. The hexagonally closed packed and surfactants for HCP pores have the affinity to naturally align parallel to the substrate making perpendicular pores more difficult to achieve (Guliants, Carreon, & Lin, 2004; D. Zhao et al., 1998).

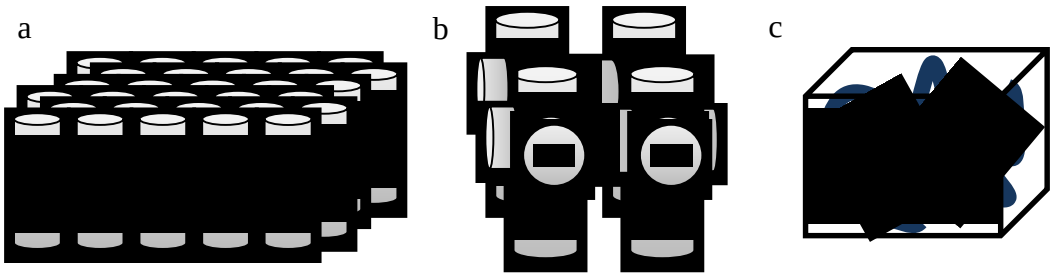

Figure 1.2. Surfactant template pore orientations a) Hexagonally Close Packed, b) Bicontinuous cubic, and c) disordered worm-like.

SILICA THIN FILMS

Silica thin films are currently being studied for advanced applications in optical chemical sensors, various filtration architectures, separations, catalysis, and solid-phase chemistry (Ariga, Vinu, Yamauchi, Ji, & Hill, 2012; Davis, 2002; Guliants et al., 2004; Jiang et al., 2013). Ceramic films and supports are being applied in these areas because of their advantages over traditional polymer membranes; they are able to withstand a variety of thermal and chemical environments in which the polymer membrane would disintegrate (Davis, 2002). A variety of sizes and shapes of silica pores have been obtained in different studies. Numerous supports have been used to synthesize these films- some playing a role in the film's orientation and other not.

Films have been prepared by three main deposition techniques onto these supports: dip-coating, casting and spin-coating (Guliants et al., 2004). Dip-coating is done by withdrawing the substrate from a homogeneous precursor solution and allowing the solution to drain to generate a film of a particular thickness. The thickness of this preparation method is primarily dependent on the rate of withdrawal of the substrate and the rate of evaporation of the solvent. Casting is done by dropping a precursor directly onto the substrate and allowing it to solidify, resulting in thicker films. Spin-coating is performed by a four stage process: deposition of the solution, spin-up, spin-off, and evaporation (Zha & Roggendorf, 1991) (Figure 1.3). The main advantage of spin-coating is that the films are typically very uniform in thickness.

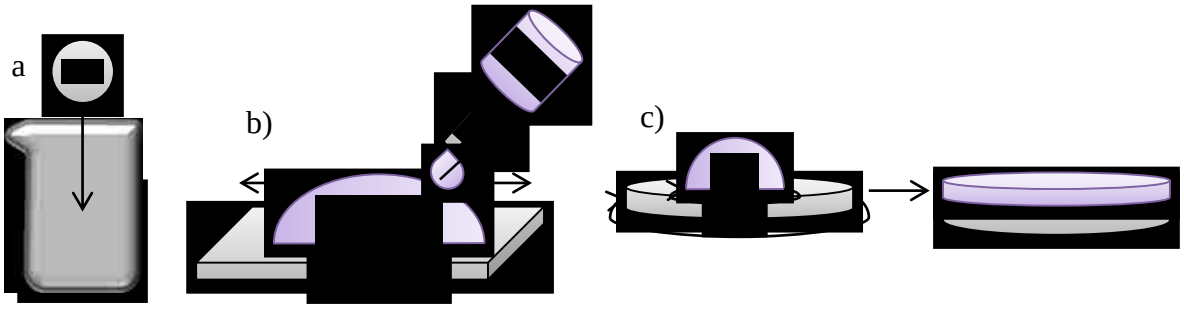

Figure 1.3. Different deposition methods on solid supports a) dipcoating, b) casting, and c) spin coating.

Polymer or surfactant pore templating also allows the silica films to achieve a desired pore size. By changing the size of the polymer, the micelles that form to template pores will also have different sizes corresponding to the polymer. Removal of the polymer leads to a void area constituting a pore throughout the thickness of the film (Zha & Roggendorf, 1991; D. Y. Zhao, Q. S. Huo, et al., 1998). This type of control is advantageous for size selective separations by being able to appropriate a specific pore size for specific separations. This method of pore synthesis also has the ability to produce nanoscale pores which result in a higher surface area, attractive for catalysis, and can be used as advanced separations of nanoscale solutes (Davis, 2002; Guliants et al., 2004).

Pores cannot be utilized for separations however, if they are not accessible for the solute to diffuse. Achieving orthogonal pores in silica films, with respect to the substrate, has shown difficult to achieve because of the tendency of cylindrical micelles to align parallel to the surface (D. Zhao et al., 1998). Many films with pores in parallel alignment have been produced and studied as optical sensors for its electrical properties as opposed to separation applications (Lu et al., 1997). Mesoporous silica films have also been used for the enhancement of proton transport to be used in fuel cells. These films were functionalized with sulfonic acid groups for higher proton conductivity. The pores were synthesized using various amounts of polymers and acid densities. The pores were found

to be ordered parallel to the substrate, which for this application is acceptable but for membranes is not usable (Fujita, Koiwai, Kawasumi, & Inagaki, 2013). Several methods exist to produce orthogonally oriented pore arrays in silica thin films, each with their advantages and disadvantages. Some methods utilize the properties of cubic structures' interconnected pore array. The pores are not solely perpendicular but are accessible to solvents and solutes. However, their interconnected pathways create longer, tortuous routes for the solutes to become trapped and accumulate.

Another method used for synthesizing nanoporous silica membranes was the use of a two-step sol-gel dip-coating route of colloidal silicas. Fuji et al. (Fujii, Yano, Nakamura, & Miyawaki, 2001) first used a fibrous silica colloid to fill the macropores of an alumina membrane followed by the deposition of silica nanoparticles therefore producing layers of particles producing a membrane. The pore sizes were found to correspond to the vacant spaces in between particles, however the surface area values found were 2-3 orders of magnitude less than reported previously (Fujii et al., 2001). This suggests that either the films have a very low porosity due to excessive aggregation or the films are very thin. The pore size can be adjusted by the size of the particles which could also be detrimental to the porosity.

Electro-assisted self-assembly (EASA) has been another method used for achieving vertically oriented mesoporous silica films (Goux et al., 2009; Platschek, Keilbach, & Bein, 2011; Platschek, Petkov, & Bein, 2006). Goux et al. showed that self-assembled hexagonally packed one-dimensional channels to grow perpendicular to the conductive substrate in the presence of an applied electrical field normal to the substrate (Goux et al., 2009). They used the lack of a peak in XRD results as evidence for the lack

of parallel alignment, but the patterns contained a small broad peak that they attributed to particles and aggregates that formed on top of the oriented mesoporous thin film. The thicker the deposition of particles on the surface the more intense the peak would become. TEM images showed the ordered pores with aggregates atop the surface even after the process was optimized. The apparent drawback of this method is the inability to deposit on a number of substrates as well as the mass transfer issues involved with depositing the layers completely inside the substrate. The more layers deposited, the more limited the mass transfer to deposit the next layer becomes.

Chemically neutral surfaces have been used to align surfactant templated pores during the sol-gel process perpendicular to a glass support (Koganti et al., 2006). Since both hydrophobic and hydrophilic surfaces yield pores aligned parallel to the surface, providing a surface where the micelle has no affinity to align parallel may lead to perpendicular alignment (Figure 1.4). A chemically neutral surface was achieved by coating glass slides in a cross linked random copolymer or block copolymer poly(ethylene glycol)-block-poly(propylene glycol)-block-poly(ethylene glycol) (P123). The pores were achieved by templating with P123 and calcining to remove the cross-linked and pore template surfactants. The thinnest silica films yielded a close packed hexagonally tilted pore orientation with a size of around 5.5 nm demonstrated by N_2 adsorption, XRD, and TEM (Koganti et al., 2006). As the films deposited by dip-coating became thicker greater than 100 nm, a parallel pore alignment became evident by XRD. This suggested the need for chemically neutral sandwiching as well. The ability to deposit a chemically neutral surface onto any surface makes this method of perpendicular pore alignment advantageous over other methods such as EASA.

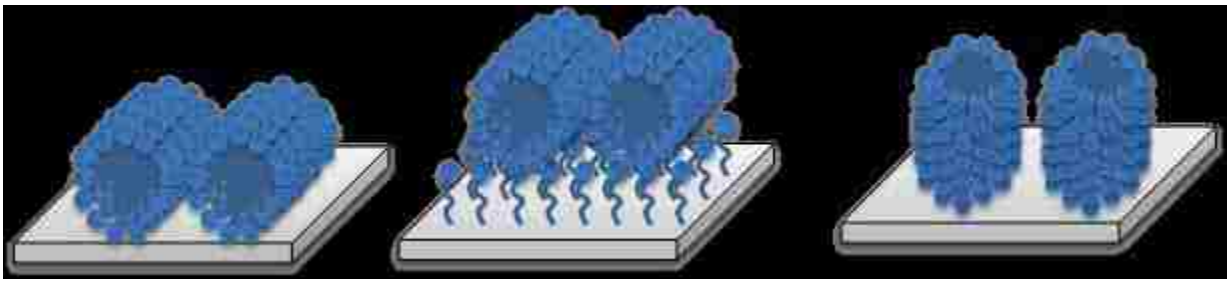

Figure 1.4. Micelle alignment on a a) hydrophilic surface, b) hydrophobic surface and c) chemically neutral surface.

SILICA FILMS ON ANODIZED ALUMINA

Silica films have been deposited onto anodized alumina supports by several different research groups. They have been studied for their ability to produce perpendicular pores by way of electrophoretic deposition for separations as described previously (Platschek et al., 2011; Platschek et al., 2006) as well as parallel pores using the sol-gel method for optimizing sensors (Markovics & Kovacs, 2013).

A previous group prepared mesoporous silica films on macroporous α-alumina supports by dip-coating method (Boffa et al., 2007). The rheology of the sol was modified by urea-based thixotropic agent to obtain ordered pores. They used surfactant templating with CTAB to create the pores. The powder form of the silica films was analyzed by XRD and N_2 adsorption. XRD results suggested that the addition of the modifying agent could be disturbing the formation of micelles which is counterproductive for making mesoporous films. According to nitrogen adsorption, pore sizes ranged from 1.8 to around 5 nm depending on the amount of modifier added; the highest concentration of modifier led to a much broader range of pore diameters compared to the lesser concentrations. Once the sol-gel was actually dip-coated onto a macroporous support, the film was seen to completely penetrate the support, not leaving a thin film of ordered mesoporous after dip-coating one time. Therefore the sol had to be coated several times onto the support in order to obtain an actual thin film. In addition, the order of the silica was never tested in the form of a thin film.

Silica has also been used as a composite membrane with AAO membranes (Maeda, Ichinose, Yamazaki, & Suzuki, 2008). An aspiration method was used whereby

the substrate was set in a filtration holder settled on a filtering flask. A needle valve connected the flask to an aspirator and the precursor was deposited for various amount of time. This method resulted in infiltration of the AAO pores by the silica which was to make smaller aligned pores. Small angle X-ray Diffraction (SAXRD) showed no peaks suggesting the pores are aligned orthogonal to the surface but further evidence is needed to support this, since the same results could correspond to completely disordered pores. The mesoporous silica layer was able to penetrate around 50 μm with a surface thickness of around 2 μm for some cases leading to a relatively thick layer of silica that has the potential to lead to mass accumulation and retardation of the membrane.

In contrast, silica membranes have also been synthesized with no support, and by simply using the sol-gel method to produce a membrane after gelation (Jiang et al., 2013). The pores obtained here are worm-like in structure but are accessible through the membrane. The pore diameter was tuned by adjusting a H_3PO_4:TEOS ratio in the sol solution. A very low flux was found for water across the membrane at an applied pressure with an average pore size of around 4 nm. This method was able to produce porous channel that met the surface of the membrane but the pores were not ordered and most had a fairly broad range of pore diameters which would not result in a specified separation process.

MATERIAL CHARACTERIZATION METHODS

Methods of materials characterization are very important in demonstrating the order and size characteristics of materials. Visualizing the pores directly using a light microsope is not feasible for nanometer scale pores. An alternative, atomic force microscopy (AFM), relies on the very slim tip of a needle-like projection to detect the surface characteristics of materials. Electron beam lithography also provides a way of cutting nanoscale material in order to make this material usable for electron microscopy.

Electron microscopy is a very important and popular technique used to view the surface and even chemical composition of materials. Scanning Electron Microscopy (SEM) uses a focused beam of electrons to view samples that are not visible in a light microscope range. Using an X-ray source, the chemical composition of the material can be observed by the interactions between the X-ray beam and the material. Transmission Electron Microcopy (TEM) is also a valuable tool in porous materials characterization. TEM uses electron beams to penetrate very thin samples in order to detect the characteristics of the material. While the sample preparation is difficult and very specific in nature, TEM is able to produce high resolution and high magnification images.

Other materials also need to be characterized based upon their thickness. If an electron microscope is not accurate enough or the sample cannot be prepared in such a way, ellipsometry is a simple way of measuring film thickness. By comparing the different chemical signature of materials, an ellipsometer is able to detect the height of a deposited layer. For example, different concentrations of silica can be deposited onto silicon wafers to measure the change in film thickness. By knowing the silicon wafer

thickness, the silica thickness can be determined by knowing the chemical properties of silica. This method typically yields more accurate results compared to other methods such as a profilometer.

Chemical composition in materials is also an important aspect of film characterization. When attaching groups to the surface of a material or attempting to remove polymer from within the pores of a material it is imperative that the composition is tested. Fourier Transform Infrared Spectroscopy (FTIR) has been used extensively for these purposes. An infrared spectrum of absorption, emission, or Raman scattering through a solid, in the form of a film or crystalized particles, is collected over a wide spectral range. Peaks in the spectra correspond to different bond stretching which signifies the presence or lack thereof a specific group or molecule.

X-Ray Diffraction (XRD) is used for characterizing material structure based on the x-ray scattering from the crystalline surface. Since many materials contain such crystalline structures, this method has a wide range of applicability. The angles and intensities of the diffracted beams can be used to determine the entire structure of the material, down to the very atom.

MEASUREMENT OF SIZE AND CHEMICAL SELECTIVITY OF MEMBRANES

Semi-permeable membranes provide a specific separation based on the size and physical characteristics of the solutes. Tailoring the pore size of the membranes can allow for a very specific size separation and mesoporous materials can be used for even nanoscale applications. While characterizing the material is important for determining the potential effects of separation, measuring the diffusion or permeability of molecules is important in observing the actual behavior of solutes in contact with materials.

Solvent flux measurements are performed by flowing ethanol or water through a membrane at given pressure drops. The time and volume of the solvent are recorded and used to calculate the solvent flux and the Hagen-Poiseuille equation, Equation 1.1, can then be applied to determine other features of the membrane:

$$J = \frac{\Delta P r^2 \varepsilon}{8 \mu L} \tag{1.1}$$

where J is the flux of the solvent, ΔP is the pressure drop through the pores, ϵ is the porosity of the membrane, r is the radius of the pores, μ is the viscosity of the solvent and L is the thickness of the membrane or length of the pores. This equation may be applied under the assumptions that the pores are cylindrical and uniform in size throughout their length, the flow through the pores is laminar, and the fluid is incompressible. If the characteristics of the membrane are available (thickness and porosity), the Hagen-Poiseuille equation can also be used to estimate the pore size of the membrane from measured solvent fluxes.

The Hagen-Poiseuille equation has been applied to model the interaction of solvents through membrane systems (Machado, Hasson, & Semiat, 2000) and the interaction of solvents with the membranes. For example, this analysis can demonstrate chemical selectivity of the membrane by measuring the flux of solvents before and after chemical functionalization of the membrane (Majumder, Chopra, & Hinds, 2011). By altering the surface energy of the membrane through functionalization, the surface tension between the solid membrane and the liquid solvent may be observed to change before and after functionalization. The relationship of surface tension and flux has been previously studied to determine the effects and modeling parameters of changing the solvents (Darvishmanesh, Buekenhoudt, Degreve, & Van der Bruggen, 2009).

For membranes comprising multiple layers, the contribution of the transport resistance in each layer to the measured flux can be described using a resistance in series model:

$$J = \frac{\Delta p}{\sum R_i} \tag{1.2}$$

where J is the flux of the solvent, ΔP is the pressure drop through the pores, and the resistance (R_i) is defined as Equation 1.3:

$$R_i = \frac{8\mu L_i}{\varepsilon {r_i}^2} \tag{1.3}$$

where ε is the porosity of the membrane, μ is the viscosity of the solvent, and r_i and L_i are the radius and thickness respectively of the particular layer being observed.

A simple apparatus to measure the diffusivity or permeability of a solute through a membrane is a diaphragm cell (Figure 1.5). This apparatus allows for the testing of solute concentrations on either side of the membrane as a function of time. Equation 1.4 (Cussler, 2009; Dullien & Shemilt, 1960) relate the concentration profile of the solute in the presence of the membrane with respect to time:

$$\ln\left(\frac{C_{D_0} - C_{R_0}}{C_D - C_R}\right) = P_i \times t \times A\left[\frac{1}{V_R} + \frac{1}{V_D}\right] \tag{1.4}$$

Equation 1.5 shows the relationship between the permeability and diffusion:

$$P_i = \frac{D_i \times \varepsilon}{l} = \frac{D_{eff,i}}{l} \tag{1.5}$$

where P_i is the permeability of solute i defined by the equation above, A is the cross-sectional area of the membrane exposed in the diffusion cell, V_R is the volume of the receptor side, V_D is the volume of the donor side, C_{D_0} is the concentration in the donor side at the previous sample time, C_{R_0} is the concentration on the receptor side at the previous sample, C_D is the concentration in the donor side at the sample time, C_R is the concentration on the receptor side at the sample time, and t is the time between samples and also where D_i is the diffusivity of solute i, ε is the porosity of the membrane, l is the thickness or entrance length of the membrane, $D_{eff,i}$ is the effective diffusivity of solute i (when the membranes have a solid porous structure). Permeability may be used instead of diffusivity when membrane characteristics such as porosity and effective pore length are unknown or cannot be accurately estimated.

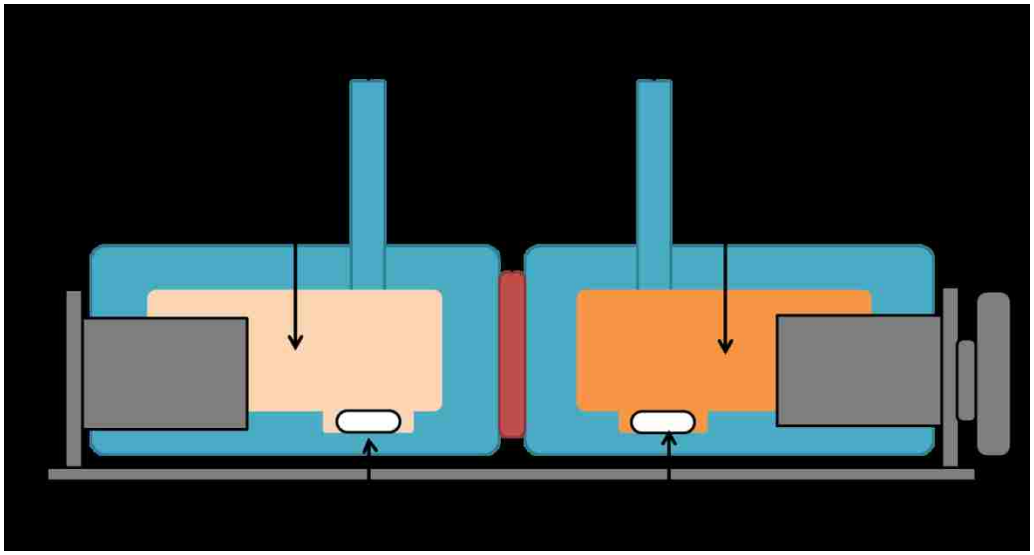

Figure 1.5. Diffusion cell used for studies the transport of various sized solutes through the membranes. Adapted from *http://www.permegear.com/sbs.htm*.

When a solute is in the presence of a porous membrane that begins to limit the diffusivity of the molecule below its bulk diffusivity, the diffusion is characterized as hindered diffusion (Deen, 1987). Several approaches exist to describe the interaction between the solutes and pores in hindered diffusion, but the Renkin equation, Equation 1.6 and 1.7, has been used frequently in its various forms in a number of studies (Deen, 1987; Hosoya et al., 2004; Johnston, Salamat-Miller, Alur, & Mitra, 2003):

$$D_{E,R} = D_{Bulk}\left(1 - \frac{Rs}{Rp}\right)^4 \tag{1.6}$$

More complex variations of the Renkin equation have also been developed to better model data such as Equation 1.7:

$$D_{E,R} = D_{Bulk}(1 - \frac{Rs}{Rp})^2(1 - 2.109(\frac{Rs}{Rp}) + 2.09(\frac{Rs}{Rp})^3 - 0.5(\frac{Rs}{Rp})^5) \tag{1.7}$$

where $D_{E,R}$ is the adjusted diffusion, D_{Bulk} is the bulk diffusion of the solute, R_S is the hydrodynamic radius of the solute, and R_P is the pore radius of the membrane. These equations have been applied for determining the change in diffusivity as a function of pore size or chemical interactions of the molecule with the pores. The latter could be due to effects of functionalizing the surface of the material.

Functionalizing the pores or surface allows for only certain types of molecules to enter, regardless of their size. Two molecules of identical size can be separated by a membrane with a chemically selective surface. Such membranes have the ability to be applied to small solute separations as well as very specific detection and purifications.

Chapter Two: THIN FILM MESOPOROUS SILICA MEMBRANES INTRODUCTION

Porous materials are currently being studied for uses in separation, catalysis, and sensing applications. Particles and films are both used for their capabilities in these areas (Nazeeruddin et al., 2006; Palaniappan et al., 2006; Ruiz-Hitzky, Darder, Aranda, & Ariga, 2010). Films are of interest in this work because of their ability to be translated into operating membranes. Traditional polymer membranes are unstable in a wide variety of environments which makes inorganic membranes attractive since they can withstand a variety of pH and temperature conditions. Porous ceramics are also readily functionalized to provide chemical separations. This coupled with the ability to determine the pores size and structure allows for the synthesis of a tailored and stable membrane system.

Current techniques for the synthesis of inorganic thin films and membranes include exposing a variety of solid nanostructured materials, used as pore framework, to metal alkoxide sol-gels (Ariga et al., 2012; Davis, 2002; Guliants et al., 2004; Jiang et al., 2013). Removal of the pore template (such as liquid crystal templates or latex) results in a controlled pore structure in the continuous ceramic film (Davis, 2002; Velev, Jede, Lobo, & Lenhoff, 1998). In the case of latex particles, the resulting thin film has a spherical and interconnected pore array, with a pore size limited by the particle size (generally approximately 50 nm to micron-sized) (Guliants et al., 2004; Velev, Jede, Lobo, & Lenhoff, 1997; Velev et al., 1998).

Electrochemical etching is another method to synthesize porous ceramic material. By etching the oxide layer of aluminum, anodized alumina membranes are produced

which are chemically and thermally robust films with large uniform arrays of cylindrical pores. This method is restricted by the difficulty in achieving a uniform size distribution is and the pore sizes being limited to between 10 nm and 100 nm. (Davis, 2002; Velleman, Triani, Evans, Shapter, & Losic, 2009). These AAO supports can be further functionalized to produce silica pores confined inside the AAO pores by electro-assisted self-assembly (EASA), achieving vertically oriented mesoporous silica films (Goux et al., 2009; Platschek et al., 2011; Platschek et al., 2006). Since the support needs to be an electrode surface, the coating method is applicable to a limited range of supports.

Surfactant templates also provide nanostructured platforms for the synthesis of porous thin films. Surfactant templated materials are of interest because of their smaller pore dimensions (between 2 and 50 nm) and their well-defined pores and orientations (Brinker, Lu, Sellinger, & Fan, 1999; Edler, Goldar, Hughes, Roser, & Mann, 2001; Edler & Roser, 2001) , which can be tailored with different surfactants, synthesis conditions, and deposition methods (Guliants et al., 2004; D. Y. Zhao, Q. S. Huo, et al., 1998). Pore structures such as cubic, worm-like, and hexagonally close packed can be achieved by varying the template, template concentration, and the synthesis conditions (Fan et al., 2007). The cubic phase results in a 3-dimensional interconnected pore array whereas worm-like pores lead to a disordered pore array. 2-Dimensional hexagonal close packed (HCP) mesophases results in non-intersecting parallel pores. The ability to control the pore orientation can be used to tailor the film to fit the need of the application.

The potential to translate surfactant templated thin film technology to membrane applications requires an accessible pore structure. Previous studies have demonstrated the ability to deposit mesoporous thin films onto porous substrates and their utilization

for membrane applications. Bicontinuous cubic phases and 3-D disordered networks provide accessible pores in surfactant templated mesoporous films. MCM 48 films, comprising a bicontinuous Ia3d cubic structure, have been synthesized on porous alumina supports. The membrane properties of these composites have been investigated by gas permeability studies (Nishiyama, Park, Koide, Egashira, & Ueyama, 2001), pressure driven solvent flow (Chowdhury, Schmuhl, Keizer, ten Elshof, & Blank, 2003), and in the separations of solvents (Park, Nishiyama, Egashira, & Ueyama, 2001, 2003). Silica thin films characterized as a 3-D disordered network were templated using cetyltrimethylammonium bromide (CTAB)) on a porous support. Gas permeation experiments demonstrated that this pore structure allowed for the diffusion of molecules through the membranes (McCool, Hill, DiCarlo, & DeSisto, 2003; Zhang, Li, Meng, Wang, & Zhu, 2003). For membrane applications, the parallel cylindrical channels of HCP pore structures have the potential advantage of lack of tortuosity and alternate paths for diffusing species relative to the interconnected pore pathways of cubic phases and wormlike thin film silica structures. However, the tendency of HCP pores is to align parallel to the substrate on which they are deposited, (Fujita et al., 2013; Lu et al., 1997; D. Y. Zhao, J. L. Feng, et al., 1998) making the pores of the composite thin film/substrate inaccessible.

Recent investigations in our group demonstrate the use of a chemically neutral surface to synthesize ordered HCP pores with an orientation perpendicular to the surface of the substrate (Koganti et al., 2006). Using P123 (polyethylene oxide (PEO)-polypropylene oxide (PPO)-PEO triblock copolymer) as a template, a chemically neutral surface was created on a glass substrate prior to dip coating the sol using crosslinked

layers of random PEO-PPO or P123 copolymers. Silica thin films templated on a neutral surface (for < 100 nm thick films) or sandwiched between two neutral surfaces (for > 240 nm thick films) have HCP pores perpendicular to the substrate surface. Without the use of neutral surfaces or above a critical thickness between 70 to 100 nm for non-sandwiched films, the orientation of the HCP pores was partially or completely parallel to the glass substrate, as interpreted from x-ray diffraction (XRD), grazing incidence x-ray scattering (GISAXS), scanning electron microscopy (SEM) and transmission electron microscopy (TEM) results. The hexagonal pores templated on neutral surfaces were designated as orthogonally tilted (o-HCP) because, while the GISAXS patterns of films cast onto glass slides shows a prominent spot in the plane of the films due to perfectly orthogonal domains, streaks extending away from these spots indicate a (narrow) distribution of tilt angles away from orthogonal (Koganti et al., 2006). This approach to the synthesis of thin films with HCP pores oriented orthogonally to the surface can be easily generalized because the crosslinked copolymer can be deposited onto any nonporous substrate, or can even be coated onto a porous substrate, to allow a continuous silica film to be deposited over the pores.

This work extends the synthesis of o-HCP thin films to porous supports, creating both a feasible ceramic membrane structure as well as platform to further test the accessibility of the o-HCP pore structure. The synthesis scheme of these thin film silica membranes is visualized in Figure 2.1. A chemically neutral surface (crosslinked PEO-r-PPO or P123) is deposited on an anodized aluminum oxide (AAO) support by dip coating. The sol gel containing the P123 template is deposited and cured on this neutral surface. Subsequent calcination is used to remove both the polymeric neutral surface and

the template, leaving an accessible pore structure. This procedure is envisioned to capture the HCP mesophase in a geometry leading to accessible, orthogonally aligned, cylindrical pores.

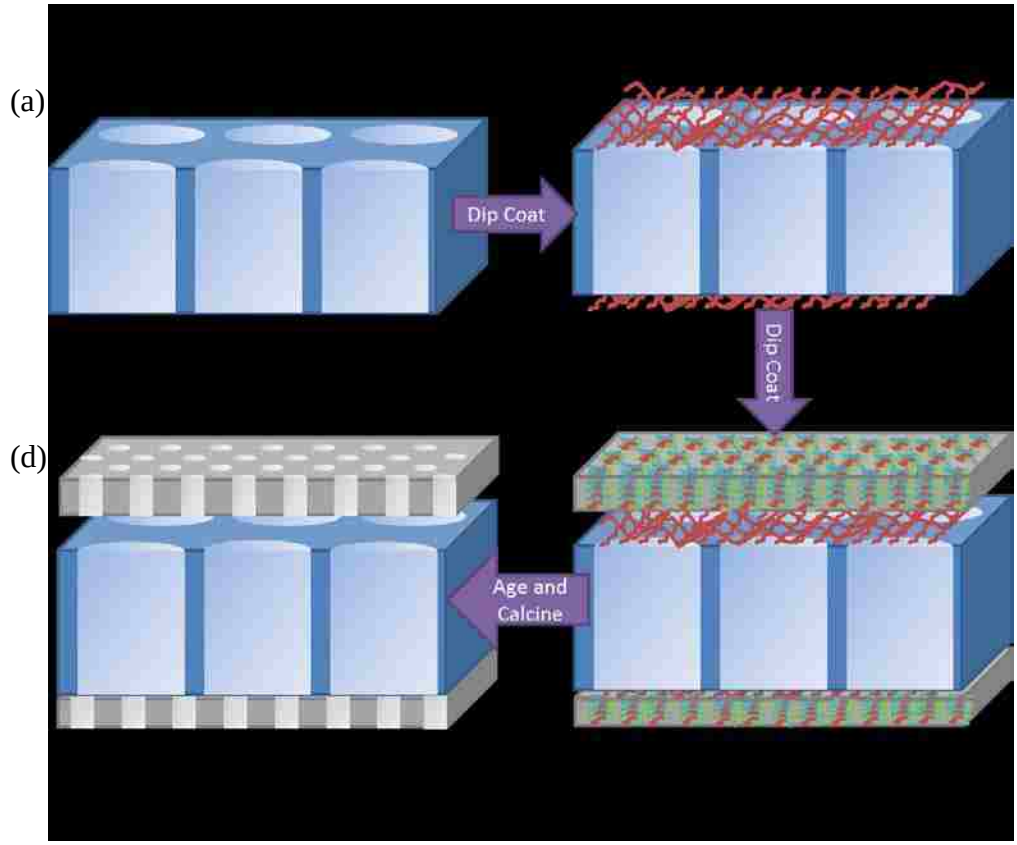

Figure 2.1. Dip coating process shown from the cross sectional view of the (a) AAO membrane; (b) AAO membrane modified with cross-linked polymer acting as a neutral surface; (c) silica thin film cast on neutral surface to achieve orthogonal pore alignment; (d) silica thin film membrane following calcination to achieve accessible pores.

This work demonstrates the pore accessibility and size selectivity of thin film silica membranes by translating the synthesis of oriented thin film silica films on neutral surfaces to porous supports. Different thicknesses of silica thin film membranes are

synthesized to demonstrate a critical thickness at which sandwiching between neutral surfaces becomes necessary to achieve accessible pore orientation. The uniformity and structure of the thin film silica layer on the AAO support is examined by scanning electron microscopy (SEM) and transmission electron microscopy (TEM), respectively. The accessibility of the pores was measured and demonstrated by pressure driven solvent flow of ethanol as a function of film thickness. The permeability of ions and fluorescently tagged solutes (5(6)-carboxyfluorescein and FITC-tagged dextrans ranging from 400 to 70,000 Da) is used to demonstrate the ability of these thin film silica membranes to separate molecules by size. This approach to synthesize pore-accessible mesoporous metal oxide membranes has the potential to be generalized to a variety of templates and macroporous supports, requiring only a neutral casting surface.

MATERIALS AND METHODS

Materials

Anodized alumina membranes (Whatman Anodisc 25) 25 mm in diameter with 200 nm pores, 0.25-0.5 porosity, and a nominal thickness of 60 μm were used as supports for the thin film silica membranes. Polyethylene oxide (PEO)-polypropylene oxide (PPO)-PEO triblock surfactant P123 (Sigma Aldrich, average Mn ~5,800) was used as a template to the pores of the silica membranes. Random copolymer PEO-r-PPO (75% EO, Mn ~12000, Aldrich) or P123 were used to produce neutral surfaces. Glycerol (Sigma Aldrich, ≥99%) was used as a cross-linker for the polymers when creating the neutral surfaces on the support. 1, 6-diisocyanatohexane (DH) (Sigma Aldrich, 98%) was used in the modification and neutralization of glass slides. Bovine serum albumin (BSA) (Sigma Aldrich, ≥96%) was used as a model protein. Fluorescein isothiocyanate–dextrans (FD-[MW]) (TdB Consultancy, Sweden) in molecular weights of 4,000 (FD4), 10,000 (FD10), and 70,000 (FD70) and 5(6)-carboxyfluorescein (CF) (Sigma Aldrich, ≥95% (HPLC)) were representative solutes with known differences in size.

Synthesis of membranes

Thin film silica membranes were synthesized on anodic aluminum oxide (AAO) supports using the thin film synthesis methods previously reported by Koganti et al. (Koganti et al., 2006). The anodized alumina membranes (Anodisc membranes with a pore size of ~200 nm from Whatman) were used as a support and were modified with P123 or random PEO-r-PPO copolymer in a dip coating process. A 0.696 mmol/L solution of P123 or 0.415 mmol/L solution of random copolymer in acetone was stirred and an equimolar amount of DH was added in a nitrogen purged glove bag. Under constant stirring, a drop of glycerol was added to the mixture. The solution was used to

dip coat the AAO membranes and to modify the glass slides used to sandwich the membranes. The dip coated supports were aged at 100°C for 24 hours to drive the isocyanate-hydroxyl reaction to completion.

Tetraethoxysilane (TEOS), anhydrous ethanol, deionized ultra-filtered water and hydrogen chloride (HCl) were added together in a mole ratio of 1: 3.8: 1: 5E-5. This solution was refluxed at a temperature of 70°C for 90 minutes. A final amount of HCl and water were added yielding a concentration of 7.34 mM HCl. The mixture was stirred at room temperature for 15 minutes. The mixture was transferred and aged at 50°C for 15 minutes. A solution of P123 and ethanol was created in a mole ratio of 0.01: 18.7 and was stirred during this time as well. The TEOS mixture was then added to the P123 mixture and was stirred for 10 minutes. The final mole ratio was 1 TEOS: 22 C_2H_5OH: 5 H_2O: 0.004 HCl: 0.01 P123. The copolymer-modified membranes were dip coated in the final solution at a speed of 7.6 cm/min.

The silica thin films on the AAO support were then sandwiched between two chemically neutral surfaces, the glass slides dip coated with a neutral polymer surface, or air-cured (non-sandwiched) on the AAO support, which also had been dip coated with a neutral polymer surface. The thin films of silica on AAO supports were aged and dried at 50°C for 24 hours and then 100°C for 24 hours. The films were then calcined in a process of heating from room temperature at increments of 0.5 °C/min to 500°C and maintained at this temperature for 4 hours. Calcination was used to remove the cross linked copolymer and the surfactant templates.

Characterization of thin films

Ellipsometry

The nominal thickness of the films were obtained by ellipsometry using a Gaertner 7109-C338G ellipsometer. The thickness was determined by measuring the thickness of films coated on silicon wafers using the same sol as was used for membrane preparation.

Electron Microscopy

Transmission Electron Microscopy (TEM) (JEOL 2010F machine) images were obtained by scraping off the thin film of silica that was deposited onto the AAO membrane and applying the scrapings to a carbon grid. Another method of preparation was to place the membrane in a 5 M HCl solution under constant stirring for 24 hours to dissolve the AAO support membrane. The resulting material was deposited onto a lacy carbon grid after being dispersed in ethanol. Scanning Electron Microscopy (SEM) images were obtained by Hitachi S 4300 SEM for bare AAO membranes with no conductive coating. The thin film silica coated membranes were imaged on a Hitachi S 900 SEM with no conductive coating as well.

X-Ray Diffraction (XRD)

XRD of the silica thin films deposited on the AAO supports was performed on a Bruker-AXS D8 DISCOVER Diffractometer at a scan rate of 1°/minute from 2θ angle of 1 to 2.5.

Pressure Driven Solvent Flow

Pressure driven solvent flow through the thin film silica membranes was used to assess accessibility of the pores. A vacuum filtration holder from Cole Parmer with a membrane size of 25 mm and filtration area of 2.83 cm^2 was secured to a 125 mL

Erlenmeyer flask attached to a Millipore chemical duty vacuum pressure pump that had adjustable vacuum pressures from 0 to 100 kPa vacuum. The volumetric flowrate of ethanol through the membrane was recorded for pressure drops of 16.9, 25.4, 33.9, or 40.6 kPa under vacuum. Similar measurements of ethanol flux through the bare AAO membrane was performed as well.

Ionic Diffusion

Ionic diffusion through the thin film silica membranes and bare AAO supports was measured using techniques described previously [32, 33]. Briefly, a 0.1 M KCl was separated by the membrane in a U-bend diffusion tube, with equal heights of fluid on each side of the membrane. A silver-silver chloride electrode was one each side of the tube. One electrode was the working electrode while the other acted as both the reference and counter electrode, where the ion concentration on both sides of the membrane can be considered the same. A constant potential of 0.6 V was applied across the cell using a Princeton Scientific Model 263A Potentiostat. The ionic current was directly measured and recorded for each membrane as a representation of the speed at which KCl was moving through the membranes. This measurement was made in triplicate using three separate AAO supports and o-HCP membranes.

Solute Diffusion

Solute diffusion through the silica thin film membranes was measured in a side by side diffusion cell (PermeGear, Hellertown, PA 18055 USA). The membrane was held into place by the chambers, which each hold 7 mL, being secured tightly together by a clamp allowing a 2 cm^2 cross sectional area of the membrane to be exposed. The donor side of the cell was loaded with 7 mL of solution with a known concentration of solute in

Potassium Phosphate buffer solution (0.9 M). The receptor side was initially loaded with 7 mL of the buffer with no solute. The concentration of solute in the receptor side and donor sides were both sampled as a function of time. Two sampling methods were used and found to yield no significant difference. One method was to take a 1 mL sample from each chamber of the cell and refill the chamber with the corresponding original solution (initial solute solution in the donor side and pure buffer in the receptor side). The 1 mL sample was then further diluted and the concentration of the solute in each chamber measured by fluorescence spectroscopy (Varian Cary Eclipse Fluorescence Spectrophotometer). An alternative method measured was to take a 1 mL sample from each side and immediately test the concentration in the spectrofluorometer. The sample was then immediately reloaded into the diffusion cell on the proper side. This method was used to avoid inaccuracies in dilutions.

Diffusion of the fluorescent solutes difluorescein isothiocyanate–dextrans (FD4, FD10, and FD 70) and 5(6)-carboxyfluorescein (CF) (376 Da) was investigated. Initial concentrations in the donor side were of 5000 ng/mL and 200 μg/mL for CF and all FD solutes, respectively. In determining the solute concentrations in the donor and acceptor solutions using fluorescence spectroscopy, an excitation wavelength of 492 nm was used for CF and 490 nm for all FDs. The height of the maximum in the emission wavelength peak over 500-600 nm was used to determine the solute concentration. Standard curves were generated with known concentrations under the same conditions resulting in an R^2 value above 0.94 for all regressions. The diffusion of bovine serum albumin (BSA) (69,000 Da) through the thin film silica membranes was measured using the Peterson assay to determine the concentration of protein in each compartment of the diffusion cell

(Peterson, 1977). The initial concentration of BSA in potassium phosphate buffer was 400 μg/mL.

A mass balance of the solutes at each sample time was used to check the accuracy of the concentration measurements and suggest if solute was accumulating on the membrane. Conservation of solute within 7% of the previous value was used as a criterion in including that sample point in the subsequent analysis of solute permeability.

RESULTS AND DISCUSSION

We have previously demonstrated the ability to control the orientation of the 2-D hexagonal (HCP) pores templated by P123 on nonporous glass and silicon substrates (Koganti et al., 2006). On unmodified glass, the synthesis process described above results in well-ordered 2-D HCP with an orientation of pores parallel to the substrate. Orthogonally tilted 2-D HCP (o-HCP) thin films were obtained by confining the 240 nm thick silica film between two "neutral" surfaces (PEO-r-PEO or P123 copolymer modified surfaces) before calcination. Thinner films (thinned by diluting the sol with various amounts of ethanol) cast onto similarly "neutral" modified glass substrates and cured in air also yielded orthogonally tilted channels when the film thickness was less than 100 nm.

In extending the synthesis of oriented silica thin films to thin film membranes, the ability to cast accessible, o-HCP silica thin films on a porous substrate appropriate as a membrane support is established. The application of the "neutral" polymer layer (cross linked random copolymer or P123) prior to dip coating is hypothesized to block the pores of the AAO substrate (0.2 um diameter) so that a continuous film of silica can be deposited (Figure 2.1). This polymer layer is removed during calcination of the thin films (which also removes the surfactant template, P123). Both methods to achieve orthogonal, accessible pore orientation on the AAO support were investigated: sandwiching "thick" films (≈ 240 nm) between two "neutral" surfaces and casting a thin film (> 100 nm) on a "neutral" surface (Konganti, 2006). Macroscopically defect-free P123-templated silica films of varying thickness were deposited onto modified AAO

membranes using the dip coating process. Evidence for either cracks or film delamination was not found visually or with an optical microscope, suggesting that continuous films are present and adhere to the AAO support even after removal of the cross-linked polymer by calcination. Ellipsometry of the sols coated on co-polymer modified silicon wafers was used to determine the thickness of the silica films.

SEM images of thin films silica deposited on AAO supports (Figure 2.2 B) are compared to AAO alumina supports without silica (Figure 2.2 A). In these plane-view SEM images, the silica coated membranes display much greater electron charging and scattering whereas the bare AAO membrane image is clearer. No defects or cracking are observed on the length scale visible in the image (~10 nm), which suggests the AAO membrane is coated with a uniform silica film. However as the film is exposed to the beam for a period of time, the film begins to tear away from the AAO pores leaving the pores bare and darker in appearance (Figure 2.2 C). Thus, it is difficult to confirm that the silica layer is defect free using this imaging technique.

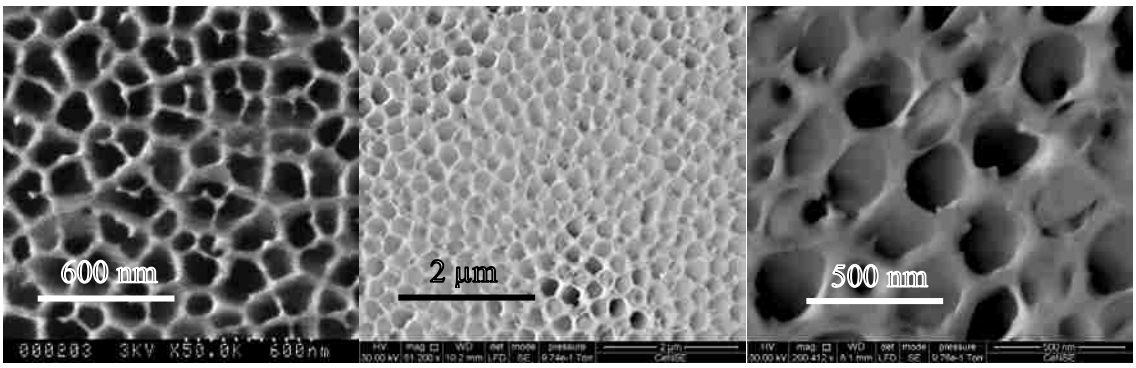

Figure 2.2. SEM images of (a) as-obtained AAO support (b) AAO support coated with silica film (70 nm thick) after calcination (Magnification: 51,200X) (c) AAO support

coated with silica film (70 nm thick) after calcination (Magnification: 200,412X) after several minutes. All images were obtained for plane-view samples.

The structure of the o-HCP layer (~ 90 nm) cast on the neutral AAO support has been examined by TEM (Figure 2.3). Although the pore structure is verified as HCP by the TEM images, TEM does not provide independent evidence of orthogonal orientation of these HCP pores to the surface of the substrate. The initial orientation of these films to the AAO surface was lost in preparing the TEM sample by scraping method. The TEM images of the silica film prepared by dissolving the AAO support (Figure 2.3) also indicate that the pores are ordered, although the desired top-view of the thin film that would confirm perpendicular pore orientation was not achieved due to curvature of the film during the preparation process.

In the case of silica thin films on solid substrates, the alignment of the pores parallel to the surface has been inferred by coupling TEM and X-ray diffraction results (Koganti et al., 2006). For ordered HCP films, parallel pores will display at least one peak in the XRD pattern whereas perpendicular pore orientations will display no peaks at all. However, a lack of XRD peaks is also consistent with a disordered material. Thus, o-HCP structure can be inferred from the observation of HCP pores in the TEM combined with a lack of peaks in the XRD. XRD of the silica thin films on the AAO support could not be obtained because the membranes did not lie flat, which interfered with the measurements.

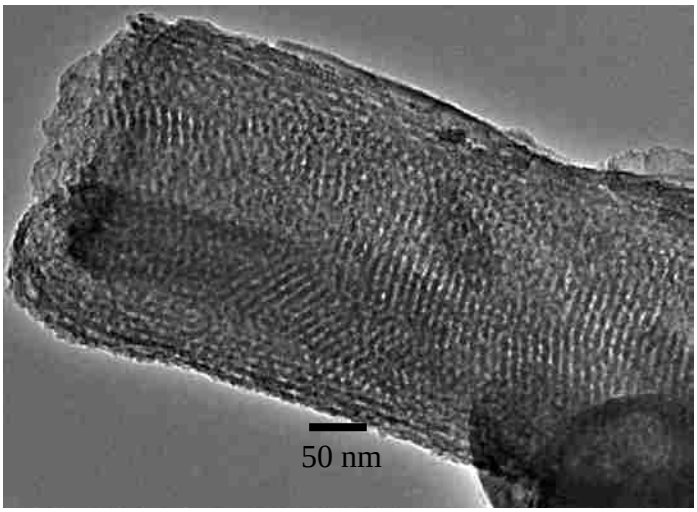

Figure 2.3. TEM image of oriented silica film after dissolving the AAO support in 5 M HCl.

Pressure driven flow of ethanol through the o-HCP silica membrane deposited onto the AAO membrane establishes the accessibility of the pores and their potential as silica thin film membranes. Ethanol flow through the membranes was measured at pressure drop ranging from 16.9 to 40.6 kPa. The flux through the o-HCP membranes is measurable, consistent with accessible pores, and is shown as a function of pressure drop for the o-HCP membranes synthesized as thin or sandwiched silica films in Figure 2.4. The flux of the bare AAO support is at least twice as great as the o-HCP silica membrane, establishing that the support also contributes to the resistance of the flow but not as significantly as the o-HCP film. As expected, the flux of the thinner membrane is greater than that of the thicker (sandwiched) membrane. The inaccessibility of pores for films synthesized at conditions resulting in pores parallel to the substrate (e.g., in the absence of neutral surfaces) is demonstrated by a flux of around 0.1 mL/min at a pressure drop of 20.3 kPa for an air-cured HCP membrane with a film thickness of about 240 nm, whereas

its o-HCP counterpart has a flux of over 1 mL/min at the same pressure drop (Figure 2.5). The linear correlation of flux and pressure drop and the reproducibility of each point suggest that the surfaces are defect free and well adhered to the support.

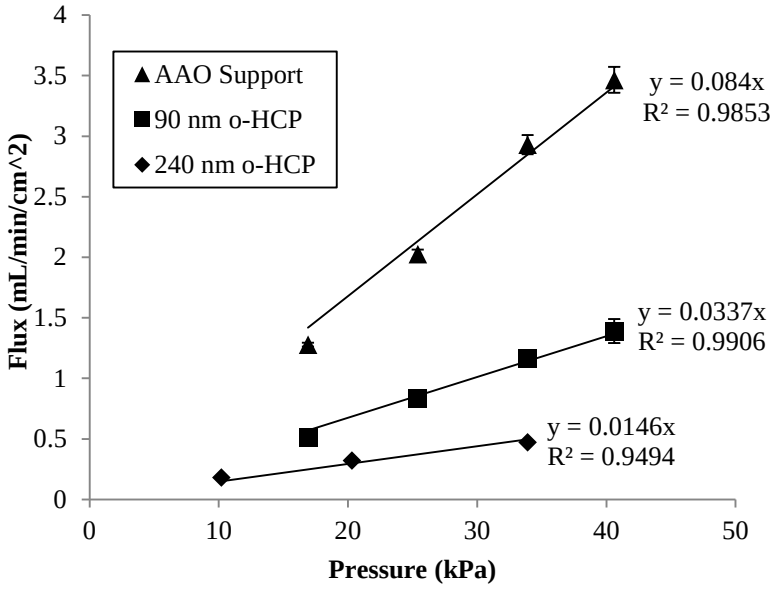

Figure 2.4. Ethanol flux vs. pressure drop across the membrane for o-HCP silica membranes of different thickness and bare AAO membrane. The lines are best fits to the data through the origin.

Solvent flux through the membrane (J) is related to the transport resistance (R) and the driving force for flow (Δp) (Equation 2.1):

$$J = \frac{\Delta p}{R} \tag{2.1}$$

The individual contribution of the AAO support layer and the silica thin films to the transport resistance can be analyzed using a resistance in series model (*Membrane Handbook*, 2001) for the composite membrane (Equation 2.2):

$$J = \frac{\Delta p}{R_1 + R_2 + R_2} \tag{2.2}$$

where R_1 is the resistance of the AAO support, and R_2 is each layer of the silica thin film. In this dip coating process, a silica thin film layer is adhered to each side of the AAO support (Figure 2.1). The silica layers are assumed to be identical.

The resistance in the AAO support, R_1, was calculated directly from the ethanol flux as a function of pressure drop for the bare support (Equation 2.3):

$$J = \frac{\Delta p}{R_1} \tag{2.3}$$

This value, 11.904 min*kPa/cm, corresponds to the inverse slope of Figure 2.4 for the AAO support. Using the transport resistance in the AAO support, the resistance in the silica thin films can be calculated from Equation 2.2. This resistance, R_2, is equal to 8.884 min*kPa/cm for the 90 nm thick o-HCP silica layer and 28.3 min*kPa/cm for the 240 nm thick o-HCP silica layer.

The resistance of the thin film silica layer of the composite membrane can be further analyzed using the Hagen-Poiselle equation (Equation 2.4), which assumes that the pores are uniform circular tubes:

$$R = \frac{8\mu L}{\varepsilon r^2} \tag{2.4}$$

where ε is the porosity of the membrane, μ is the viscosity of the solvent, r is the pore radius, and L is the length of the tube. The pore radius of the o-HCP layers can be estimated from Equation 2.4. The pore length is approximated as the nominal thickness of the film. The porosity of the o-HCP films was calculated to be 0.5 based on the measured refractive index of the films (Konganti, 2006). From the resistances, R_2, of the thin film silica layers, the estimate of the pore diameter is 10.8 nm for the thinner (90 nm thick) o-HCP films and 10 nm for the thicker (240 nm thick) o-HCP films. Solvent flux data on the bare AAO support was used to confirm a porosity in the range of the manufacture's specification by the use of the Equation 2.4.

In comparison, a pore diameter of 5.4 nm was measured by nitrogen adsorption for P123 templated thin silica films with parallel HCP pore orientation deposited on and then scraped from glass substrates (Koganti et al., 2006). For the identical sol deposited on glass substrates, the d-spacing of the (100) peak in XRD patterns of parallel oriented pores is 5.5 nm (Koganti et al., 2006). The corresponding pore diameter is therefore slightly less than 5.5 nm (after subtracting the estimated wall thickness from the unit cell parameter) (Koganti et al., 2006). In the absence of an XRD peak for o-HCP films, there are not comparable measurements for the pore size of P123 templated o-HCP silica films. However, the templating of o-HCP titania films using P123 has recently been achieved through the neutral surface templating approach used in this work (Das et al., 2014). The SEM imaging of titania films is much simpler because of the electronically conductive properties of titania relative to silica, which is an insulator and charges in the SEM. SEM imaging has been used to confirm both o-HCP orientation (using the pore structure from the plane view) and o-HCP pore diameter of ~10 nm, with a 14 nm unit cell parameter.

25% contraction of the unit cell of the HCP structure in the films with parallel to the substrate observed prior to calcination, and additional contraction upon calcination may explain the difference between the pore diameter reported by Koganti and suggested by the flux measurements. The 14 nm unit cell parameter was observed to be stable in orthogonally oriented pores after calcination (Das et al., 2014).

Ethanol flux is also used to demonstrate the ability to switch between accessible and inaccessible pores based on film thickness and sandwiching between neutral surfaces. In Figure 2.5, ethanol flux is reported as a function of film thickness for films deposited on a neutral crosslinked polymer surface and cured in air (unsandwiched films). The ethanol fluxes predicted by the resistance in series model (Equation 2.2) is also plotted using the parameters determined for the o-HCP silica thin film membranes. The resistance in the o-HCP silica thin film layer was described using the Hagen-Poisseulle equation (Equation 2.4), a pore diameter of 10 nm, and the variable film thickness as the length, L. The ethanol flux decreases with increasing film thickness in a manner predicted well by the resistance in series model at thicknesses of 50 and 70 nm in the unsandwiched films. However, the unsandwiched membranes with 126 nm thick silica film has significantly less flux than predicted, and the 240 nm silica film has negligible flux. In contrast, ethanol flux through the 240 nm silica film membrane synthesized by "sandwiching" between neutral surfaces is measurable and returns the flux to the predicted values for this film thickness. The flux results suggest that exceeding a critical film thickness in air-cured membranes shifts the structure of the pores from accessible to inaccessible. This is consistent the previous investigation of P123 templated silica thin films on neutral-coated glass slides (Koganti et al., 2006), which demonstrate a critical

thickness around 100 nm, as indicated by the appearance of an XRD peak consistent with parallel pore structures above 100 nm. In addition, sandwiching the silica films between two chemically neutral surfaces is necessary to obtain accessible pores with increasing film thickness, which is also consistent with the synthesis of o-HCP silica thin films on nonporous substrates. (Koganti et al., 2006)

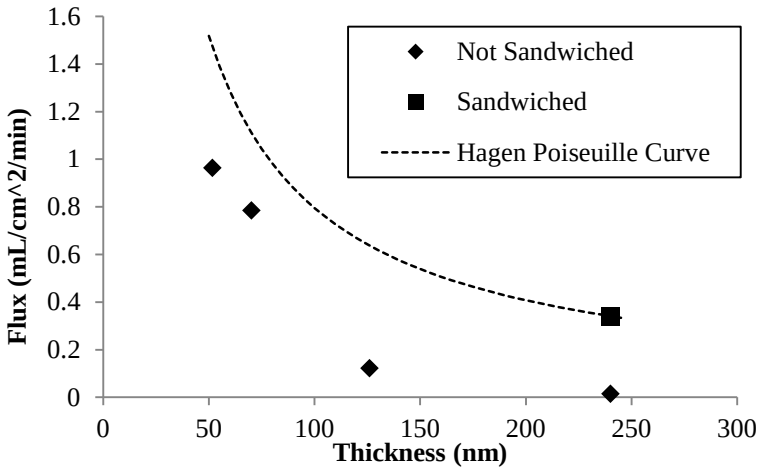

Figure 2.5. Ethanol flux as a function of thin film silica membrane thickness at a fixed pressure drop of 20.3 kPa. With the exception of the "sandwiched" point, all data were obtained for silica films cast onto AAO substrates coated with a chemical neutral surface. The curve is the prediction of the resistance in series transport model (Equation 2.2), using the Hagen-Poiseulle equation (Equation 2.4) to describe the resistance of the silica thin films.

Solute diffusion studies demonstrate the size selectivity of the membrane, the accessibility of the pores, and the absence of defects on the surface. The permeability of silica thin film membranes (nominally 90 nm thick, synthesized by sandwiching between neutral surfaces) to ions and solutes of increasing size was measured and compared to the

permeability of the bare AAO support. Different sized molecules (Table 2.1) were chosen to demonstrate the size selectivity characteristics of the silica film. The use of fluorescently-labeled dextrans of increasing size allows the comparison of size selectivity for molecules with similar interactions with the membrane surface. The approximate Stoke's radius of each molecule was calculated from its bulk diffusivity.

Table 2.1. Molecules used for diffusion experiments with corresponding molecular weight and Stoke's radius.

Molecule	Molecular Weight (Da)	Stoke's Radius (nm)
5-6 Carboxyfluorescein (CF)	376	0.63
Fluorescein isothiocyanate–dextran (FD4)	4,000	1.40
Fluorescein isothiocyanate–dextran (FD10)	10,000	2.36
Fluorescein isothiocyanate–dextran (FD70)	70,000	5.8
Bovine serum albumin (BSA)	69,000	6.45

Diffusion of ions through the AAO support and o-HCP silica thin film membranes was measured directly as the current through the membranes for a 0.1 M KCl solution in a u-bend diffusion cell. The ionic current is representative of the velocity at which the KCl diffuses through the pores of the specific membrane. The ionic diffusion within the bare AAO support yielded a KCl ionic current of 1.32 ± 0.41 μA whereas the o-HCP films deposited onto the supports yielded 1.10 ± 0.39 μA. The uncertainty of the measurements is too large to determine if the silica thin film layer adds additional resistance to transport in the composite membranes. Similarity in the transport of small ions between the bare AAO support (200 nm diameter pores) and the silica thin film

membranes is not unexpected, particularly for silica film pores in the range of 10 nm diameter.

The diffusion of solutes is reported for several o-HCP silica thin film membranes (labeled **1-3;** nominal thickness of 90 nm), with a goal of demonstrating consistency between membranes. The diffusion of the small solutes (CF, FD4, FD10, and FD70) was measured using a single membrane, while separate membranes were used for the larger molecules (BSA) to ensure mass accumulation in the pores did not reduce diffusion. Figure 2.6 shows the concentration profiles of the small solutes in the acceptor cell for the bare AAO support and one o-HCP silica thin film membrane. The percentage of the total solute that has diffused through the silica thin film membrane at 2.75 hours, as determined from direct sampling and replacement of the contents of the diffusion cell chambers, indicates that the small molecules diffuse through the membrane more readily (32.2% of CF, 12.5% of FD4, and 11.7% of FD10). Minimal diffusion of FD70 (Stoke's radius of 5.8 nm) is observed, and solute that is observed to pass through the membrane may represent the smaller molecules in the FD70 weight distribution. In addition, a model protein, BSA was measured at specified times on both the donor and receptor side of the AAO support. BSA was seen to permeate through the AAO pores over a 24 hour period, increasing the receptor concentration and decreasing the donor side concentration. BSA did not diffuse through the o-HCP silica thin film membranes after 24 hours, showing a size cut off of Stoke's radius around 6 nm for the o-HCP film. The concentration of BSA on the donor side was also measured in the silica thin film membranes; this concentration was unchanged over the course of the experiment. This supports the idea that the protein is not simply sticking to the membrane. The lack of

diffusion of BSA, whose Stoke's radius is larger than the estimated radius of the silica pores (5 nm) is further evidence that the membrane is mesoporous and defect free.

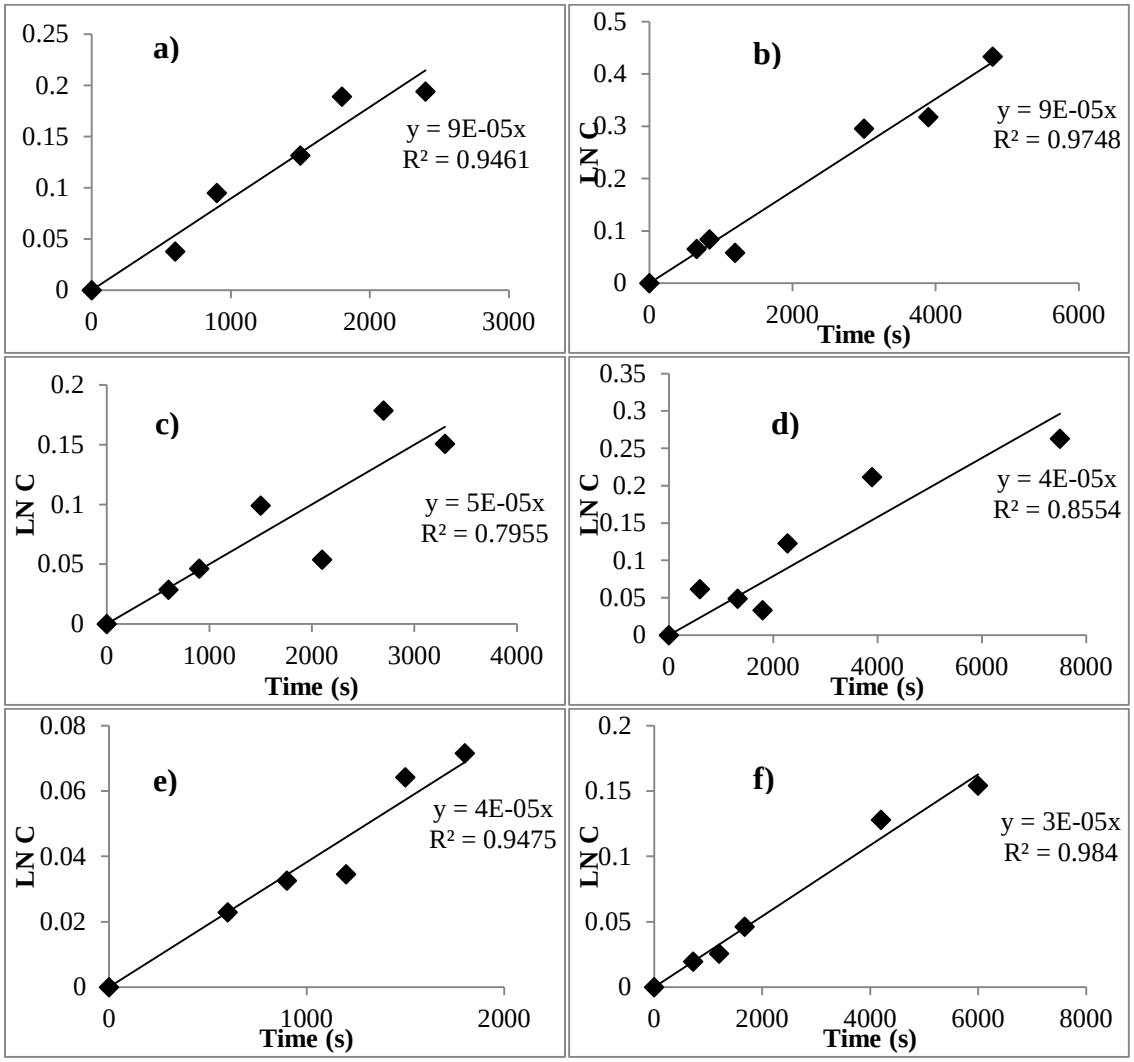

Figure 2.6. The concentration profiles ($\ln\left(\frac{C_{D_0}-C_{R_0}}{C_D-C_R}\right)$) vs. time graphs used to determine permeability of the solutes for a) AAO support with CF, b) o-HCP 3 membrane with CF, c) AAO support with FD4, d) o-HCP 3 membrane with FD4, e) AAO support with FD10, and f) o-HCP 3 membrane with FD10.

The permeability of each solute was calculated from the solute concentration on each side of the diffusion cell as a function of sampling time (Equation 2.5) (Cussler, 2009):

$$\ln\left(\frac{C_{D_0}-C_{R_0}}{C_D-C_R}\right) = P_i \times t \times A\left[\frac{1}{V_R}+\frac{1}{V_D}\right] \quad (2.5)$$

where P_i is the permeability of solute i, A is the cross-sectional area of the membrane exposed in the diffusion cell (~2 cm^2), V_R is the volume of the receptor side (7 mL), V_D is the volume of the donor side (7 mL), C_{D_0} is the concentration in the donor side at the previous sample time, C_{R_0} is the concentration on the receptor side at the previous sample, C_D is the concentration in the donor side at the sample time, C_R is the concentration on the receptor side at the sample time, and t is the time between samples. Permeability was calculated from the slope of the linear plot of the $\ln\left(\frac{C_{D_0}-C_{R_0}}{C_D-C_R}\right)$ versus time using the constant cell parameters (A_C, V_R, and V_D) (Figure 2.6). The permeabilities as a function of corresponding molecule's Stokes radius is shown in Figure 2.7 with the standard error obtained from linear regression analysis. The three o-HCP membranes synthesized under identical conditions yielded similar permeability, where the permeability decreased with molecular size in the series CF, FD4, and FD10. The bare AAO support also provided some resistance to diffusion of the solutes, but the permeability of the solutes was greater in the AAO support than in the silica thin film membranes. The o-HCP silica films did not significantly hinder the diffusion of the smallest solutes. However, it enhanced the size selectivity of the membranes as the size of the dextrans became larger. The relative thickness of the layers of the composite

membrane may account for the minimal enhancement of size selectivity by the silica layer; the AAO support is 60 μm while each silica layer is approximately 90 nm.

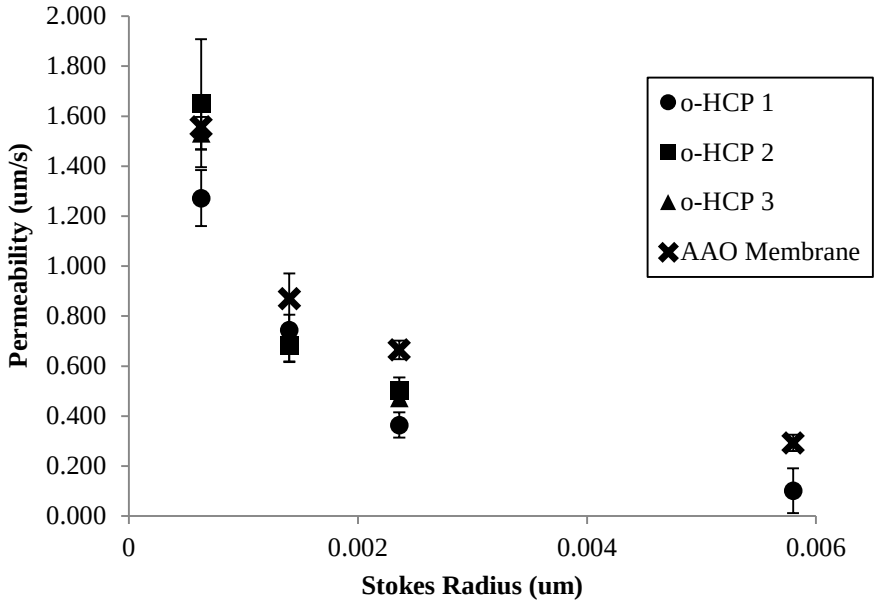

Figure 2.7. Permeability of CF, FD4, FD10 and FD70 (as a function of their Stoke's radius) o-HCP silica thin film membranes (90 nm thick) synthesized under identical conditions (o-HCP **1-3**) determined from regression analysis.

The contribution the AAO support and silica thin film layers to resistance to solute diffusion can be described by a resistance in series model that is used to quantify the resistances of each layer (Equation 2.6):

$$P_i = \frac{1}{R_{D1} + R_{D2} + R_{D2}} \tag{2.6}$$

where P_i is the permeability of a specific solute molecule through a membrane, R_{D1} is the resistance of the support for diffusion of solutes, and R_{D2} is the resistances of each of the silica films deposited on both sides of the support (assuming they have

identical transport properties). R_{D1} for each solute was calculated as the inverse of its permeability through the bare AAO support. Figure 2.8 shows the diffusional resistance of the o-HCP thin film layer for each of the solutes as calculated for several membranes. Size selectivity of o-HCP thin film layer is demonstrated by the increase in diffusional resistance with molecular size.

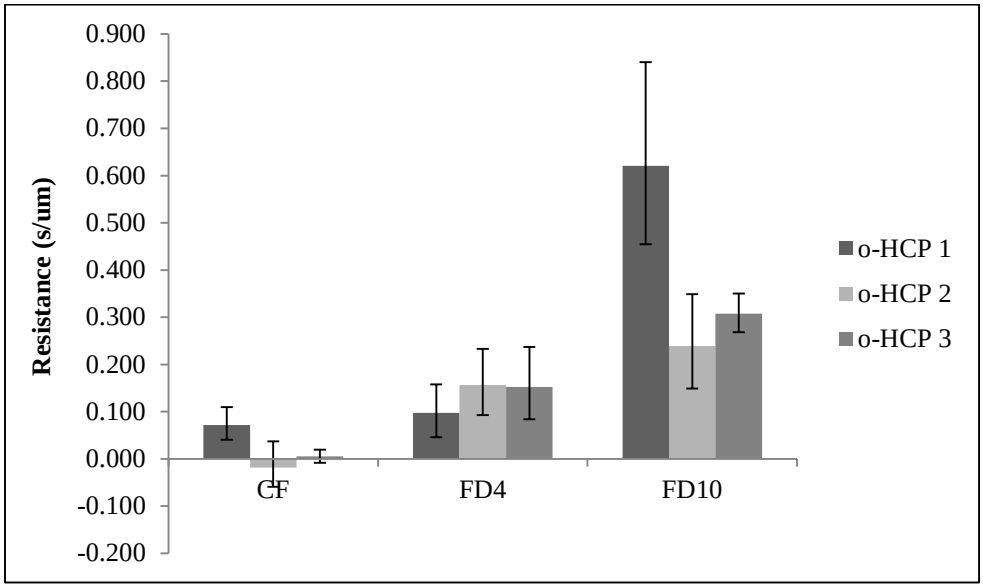

Figure 2.8. Resistance of the silica layers of the o-HCP membranes for CF, FD4, and FD10.

The reusability of the membranes **o-HCP 1-3** was demonstrated following the diffusion of CF, FD4, and FD10 through the pores. The membranes have 82-89% of the original ethanol flux. The measurement was made without cleaning the membranes and suggests the flow through pores was not significantly retarded by the accumulation of solute. This is a promising result may be enhanced with cleaning procedures.

One issue that may arise in nano-porous structures is the adsorption of the diffusing solute on the the surface of the membrane. In the diffusion experiments, mass

accumulation on the membrane surface would lead to an apparent decrease in the total mass of solute in solution. Therefore, mass accumulation demonstrates the absorption capacity of the membrane in the presence of the different molecules. The mass balance for CF showed no statistical evidence for accumulation on the membrane, however an apparent decrease in total mass in solution was observed for FD4 (14% decrease) and FD10 (17% decrease) during the first two hour of exposure to the silica thin film membranes. These data points taken before the adsorption occurred were not used in the corresponding permeability calculations because they did not satisfy our mass balance criteria. Because the permeability was calculated using solute concentrations measured at each sampling time (and not relying solely on the initial donor cell concentration of the solute), solute permeabilities could be calculated when additional mass depletion due to adsorption was negligible. In the case of size exclusion membranes, solute adsorption could be problematic. Reducing the interaction of the solute with the surface could be achieved by functionalizing the silica layer of the membrane. Conversely, chemically selective membranes require an affinity of the solute for the membranes. This could also be achieved by functionalizing the silica layer of the membrane.

CONCLUSION

Demonstrating pore accessibility is critical in extending the previous observation of orthogonal oriented silica thin films cast on nonporous substrates to the synthesis of membranes on porous supports. Accessible, HCP silica thin films consistent with an orthogonal orientation were successfully synthesized on a porous substrate (AAO membranes) by casting onto chemically neutral surfaces. Thinner films (less than 100

nm) were oriented perpendicular by air-curing but for thicker films it was found that sandwiching between two chemically neutral surfaces was necessary. Solvent flux experiments were used to estimate a pore diameter of 10 to 11 nm depending on the film thickness. This pores size is significantly larger than previously measured for P123-templated HCP pores with parallel orientation to the substrate surface, but consistent with s o-HCP titania films templated using P123 on neutral surfaces. Diffusing small molecules of varying sizes were used to demonstrate the size selectivity of the o-HCP silica layer of the composite membrane. The permeability of the membrane decreased with increasing solute size. The corresponding contribution of the silica thin film layer to diffusional resistance also increased with solute size. Size cut-off occurred around 69,000 Da seen by the lack of permeation by the model protein, BSA. The integrity of the silica thin film structures was demonstrated by its reproducible size selectivity and its reusability.

This synthesis approach to thin films silica membranes is applicable to a range of templates and supports, requiring only a neutral surface to alter pore alignment. The functionalization of these membranes can be used to further reduce interactions between the solute and the membrane for size selective separations or provide chemical selectivity to the membrane. The synthesis of pore accessible metal oxide thin film membranes has the potential to contribute to separation, catalysis, and sensing applications within the framework of the rapidly advancing field of mesoporous metal oxides.

Chapter Three: Functionalized Silica Thin Films
INTRODUCTION

Mesoporous silica thin films are of interest for a variety of applications including small molecule recovery, detection of chemicals, and waste removal (Ariga et al., 2012; Davis, 2002; Yoshitake, 2005). These types of materials provide chemical and thermal stability in a variety of environments making them more attractive over traditional polymer membranes thin films. The small pores of the films allow the stable interface to interact with small solutes and potentially filter out larger ones in a process of size selection. An additional advantage of silica thin films is the ease of functionalization, either by including organic-functionalized precursors in the initial sol (direct synthesis) or post-synthesis functionalization using reactive precursors (Vinu, Hossain, & Ariga, 2005).

In order to provide chemical selectivity to the thin film silica membranes, the silica films were functionalized with a long chained alkyl group using established techniques for mesoporous silica (Berlier et al., 2013). The thin film silica membranes were synthesized by deposition of P123 templated silica on an AAO support with a P123 modified chemically neutral surface. As described in Chapter 2, these membranes are approximately 10 nm in pore diameter and have 90 nm thick silica films. Functionalization was achieved using post synthesis grafting using n-decyltriethoxysilane (D-TEOS) precursor, and the thin films were characterized before and after functionalization. Fourier Transform Infrared Spectroscopy (FTIR) was performed on the membranes at each point in the synthesis of the silica thin film membranes (for the bare AAO support; silica-coated membrane on polymer coated AAO support as cast;

calcined thin film silica membranes; and functionalized thin film membranes). The characteristic peaks of chemical stretching were used to determine the presence of the alkyl group. Functionalization of the thin film silica membranes with the long chain alkyl group resulted in a hydrophobic surface. The contact angle of DI water on the thin film silica membranes was used to evaluate the hydrophobicity of the surface before and after functionalization. Pressure driven solvent flux was performed using both ethanol and water before and after functionalization to demonstrate the hydrophobic nature of the membranes but also to ensure that the nano-scale pores were not blocked by the functional group.

MATERIALS AND METHODS

Materials for synthesizing the membranes are identical to those in Chapter 2. The precursor to the decyl functional group, n-decyltriethoxysilane (D-TEOS), was purchased from Gelest, Morrisvilled PA. ACS grade anhydrous toluene (>99.8%), used as a solvent in the functionalization, was purchased from Sigma Aldrich.

Synthesis of the silica thin films on AAO supports was performed by sol-gel synthesis as described in Chapter 2. The membranes are expected to have a pore diameter of approximately 10 nm. The nominal thickness of the silica film deposited onto the AAO film was 90 nm. The pore orientation was to be hexagonally close packed and orthogonal to the surface of the support.

The calcined membranes were functionalized with a long alkyl chain using post-synthesis grafting methods. The method for functionalizing the o-HCP membrane with decyl groups was adapted from previous literature (Berlier et al., 2013). Calcined membranes (diameter of 25 mm) were placed in a glass dish with 30 mL of toluene. A lid was loosely placed on the dish after 0.8 mL of n-decyltriethoxysilane (D-TEOS) was added drop-wise. This was left to react for six hours under gentle mixing before removing the membranes and placing them in an oven at 100ºC to complete the reaction overnight. The membranes were then thoroughly rinsed with ethanol four times. For comparison, bare AAO membranes were also allowed to react in the mixture. All tests with functionalized membranes were completed after this step.

Contact angles of DI water on the surface of functionalized and non-functionalized o-HCP membranes were performed using a contact angle goniometer (Rame Hart). The advancing contact angle was measured by gradually dropping the liquid onto the sample until the angle no longer changed. This angle was recorded as the contact angle for the sample and solvent used.

Fourier Transform infrared spectroscopy (FTIR) was performed on a ThermoNicolet Nexus 470 using a thin film holder. A deuerated Tri Glycine Sulfate (DTGS) detector was used with a constant CO_2 stream input. The same membrane was used throughout the entire process from beginning substrate (bare AAO membrane), after sol-gel coating but before calcination, post-calcination, and post-functionalization. An AAO membrane that was exposed to the D-TEOS/toluene solution under identical reaction conditions as the o-HCP membranes was also examined by FTIR. A resolution of 8 was used with an aperture of 100 and 300 scans. The sample compartment was purged for 5 minutes before taking a reading.

Pressure driven solvent flux was analyzed before and after functionalization of the o-HCP membranes or AAO supports. A vacuum filtration holder from Cole Parmer with a membrane size of 25 mm and filtration area of 2.83 square cm was secured to a 125 mL Erlenmeyer flask attached to a Millipore chemical duty vacuum pressure pump that had adjustable vacuum pressures from 0 to 100 kPa vacuum. The volumetric flowrate of ethanol through the membrane was recorded for pressure drops of 16.9, 25.4, 33.9, or 40.6 kPa under vacuum. The flow of solvent through the membrane was measured from the time a known volume of solvent passed through the membrane at a fixed pressure drop. Different solvents (ethanol, water and hexane) were used to compare the effects of

the surface hydrophobicity of the membrane before and after functionalization on solvent flux. Different solvents, including ethanol and hexane, have been used previously in PDMS membrane systems to determine the transport properties of the solvents and membrane making this technique applicable (Postel, Spalding, Chirnside, & Wessling, 2013; Robinson, Tarleton, Millington, & Nijmeijer, 2004). Deionized water represents a highly polar compound; ethanol was used for its relative neutrality and hexane was examined for its hydrophobicity. After each membrane was situated into the holder, 3 mL of the chosen solvent was flown through at four different pressures, 5, 7.5, 10, and 12 in. Hg. Each pressure was repeated in triplicate. Solvent flux was measured through in bare AAO supports (before and after functionalization) and o-HCP thin film silica membranes (before and functionalization). This was done to demonstrate the increased effect the functionalized silica has over the functionalized AAO.

RESULTS AND DISCUSSION

The hydrophobic property of the functionalized membrane was tested using contact angle measurements with DI water. The measurements were conducted before and after functionalization. The pre-functionalized o-HCP membranes in the presence of water yielded a contact angle of 5º while the decyl functionalized o-HCP (D-o-HCP) membrane had an angle of 145º. The contact angle for the AAO membranes before and after functionalization was 35º and 135º respectively. Ethanol spread readily on the surface of all the membranes tested, so a contact angle could not be measured. The difference in contact angle between the pre and post functionalized membranes using water shows the drastic change the presence of the decyl groups provide. The contact angle of the post-functionalized o-HCP membrane (145º) makes it nearly a "super hydrophobic" material which would display a contact angle of 150 º or above (Feng et al., 2002). This demonstrates the nature of membranes after they have been functionalized with the long chained alkyl groups. Other studies have used these measurements in a model of membrane transport for resistance in series making this measurement relevant for solvent flow observations as well (Machado et al., 2000). Contact angle measurements describe the surface tension between the solid membrane surface and liquid solvent. The difference in surface energy obtained has been shown to change the flux of different solvents through the membrane system since convection through the pores is altered by the interaction of the solvents with the outer surface of the membrane and the pore walls (Darvishmanesh, Buekenhoudt, et al., 2009). The drastic change in contact angle suggests that the flux will also be changed for water here.

The FTIR spectra seen in Figure 3.1 displays the entire spectra for the o-HCP samples taken of the same membrane throughout the synthesis process. Table 3.1 shows the characteristic absorption frequencies for the relevant chemical bonds. The absorption bands corresponding to Al-O-Al and Si-O-Si and Si-OH bonds, measured directly from the thin films and not obtained as KBr pellets, are consistently seen to have an extremely high peak value that is above the detection limit of the instrument. The clear presence of silica is demonstrated after sol-gel dip coating. Before calcination, the polymer is still in the pores and on the surface of the membrane which is seen in Figure 3.2 by the presence of CH_2 stretching (stretching seen from 3000-2800). After calcination and before functionalization there is no longer any indication of the C-H stretching. After functionalization of the membrane, the C-H stretching is once again present due to the decyl groups. Since the C-H stretching is absent after calcination, it can be ruled out as the reason for the presence of this peak after functionalization. Presence of these peaks illustrates the presence of the functional group but does not prove the attachment of them onto the surface of the membrane.

Table 3.1. Characteristic FTIR absorption frequencies and corresponding bond vibrations

Type of Bond	**Wavenumber (1/cm)**
Si-OH Stretching	1060-980
Si-O-Si Stretching	1200-1080
Alumina oxide	~1110 and ~960
C-H Stretching	3000-2800

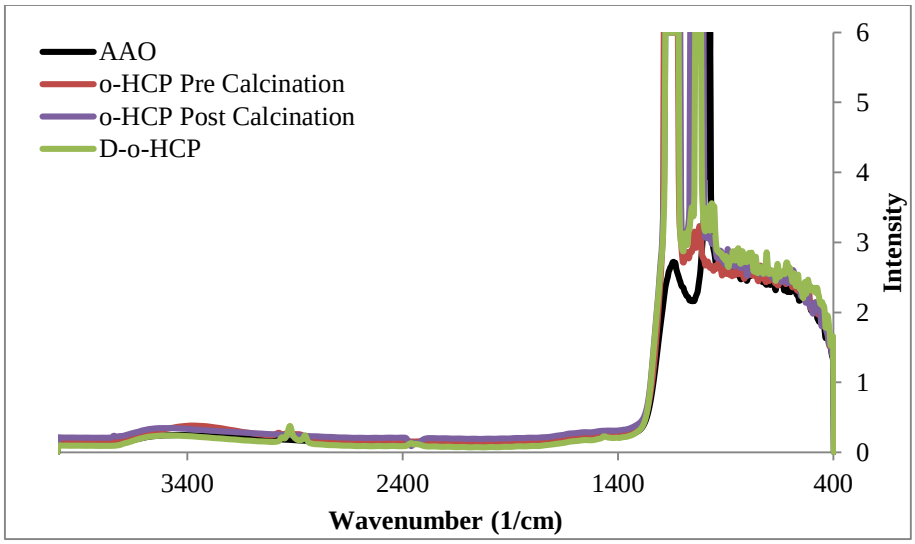

Figure 3.1. FTIR spectra for the bare AAO support, the o-HCP membrane before removing the polymer template by calcination, o-HCP after removing the polymer by calcination (finished o-HCP membrane), and decyl functionalized o-HCP membrane (D-o-HCP).

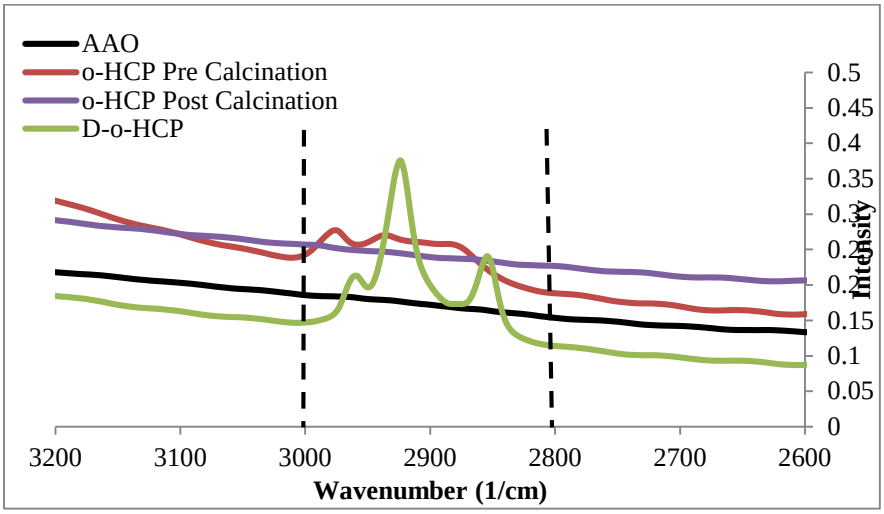

Figure 3.2. Segment of FTIR spectra for the o-HCP membranes from AAO to functionalized with decyl groups. The characteristic absorption frequency for C-H stretching is marked by the dotted lines.

FTIR was also used to analyze the bare support before and after functionalization with the decyl groups (Figure 3.3). No C-H stretching is present before the addition of the decyl as expected, however after functionalization a band does exist in the C-H stretching range (Figure 3.4). This peak has the same characteristic features as the functionalized o-HCP membrane shown in the same graph. However, the functionalized o-HCP membrane is seen to have a significantly higher peak due to the heightened presence of the decyl on the o-HCP layer as compared to the bare support (Figure 3.4). This result is promising in regards to selective functionalization. The increase of C-H stretching suggests that not only has the support been functionalized but the thin film itself has also been modified.

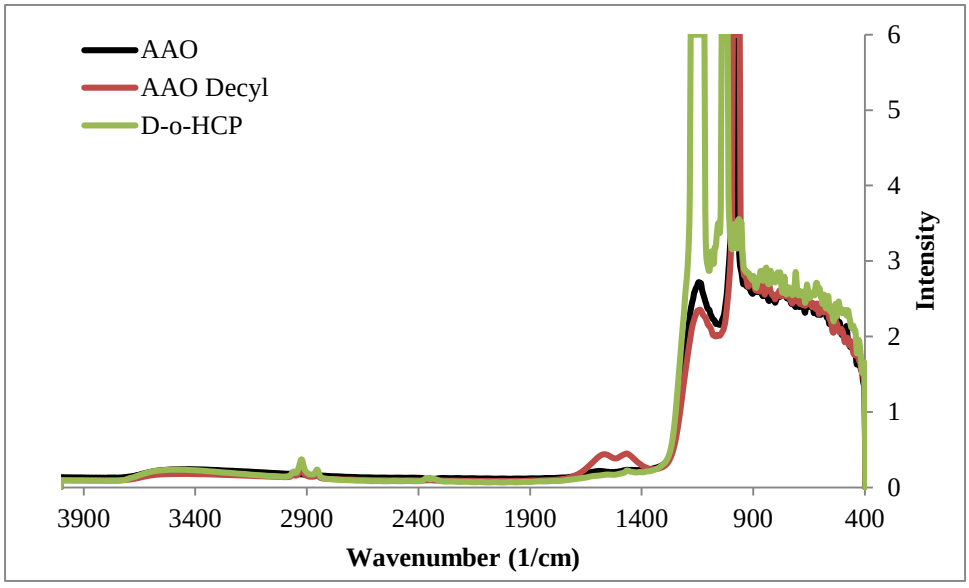

Figure 3.3. Full FTIR spectra for the AAO and o-HCP membranes after functionalization with decyl groups.

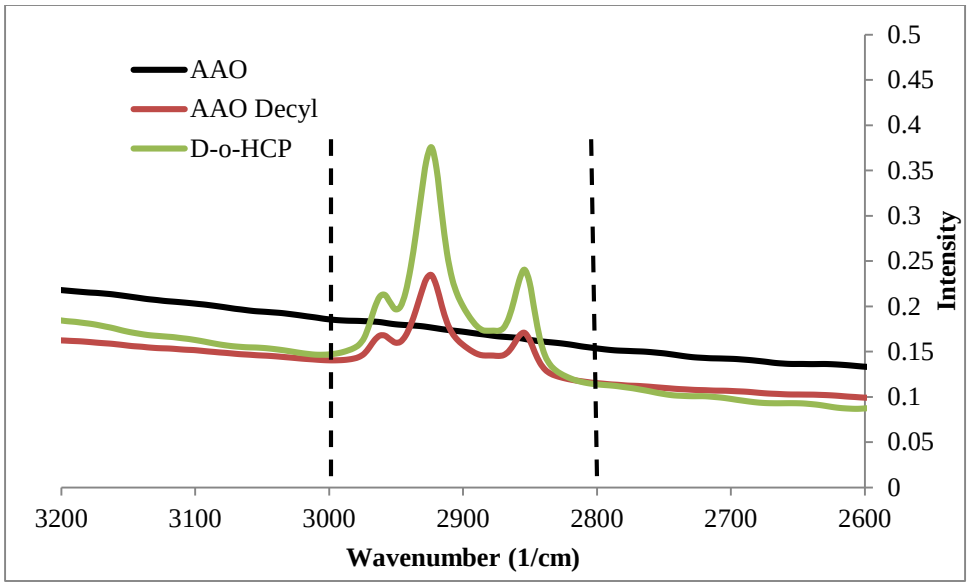

Figure 3.4. Segment of the FTIR spectra for the AAO support and o-HCP membrane after functionalization with decyl groups. The characteristic absorption frequency for C-H stretching is marked by the dotted lines.

Functionalization of the bare support and the o-HCP membranes with decyl groups affects the pressure driven solvent flux of water and ethanol. The flux of hexane was also investigated, but flow was very high (from 30-40 mL/min for the pressures used) and resulted in a high uncertainty in the experimental measurements. The functionalization of the AAO membrane yielded variable results between the solvents (Figure 3.5). Although there is an apparent increase in flow of ethanol after decyl functionalization of the AAO support, these differences are within the uncertainties of the measurements over some of the pressures. Functionalization decreases the water flux through the AAO support more significantly, consistent with the presence of the decyl on these membranes as well.

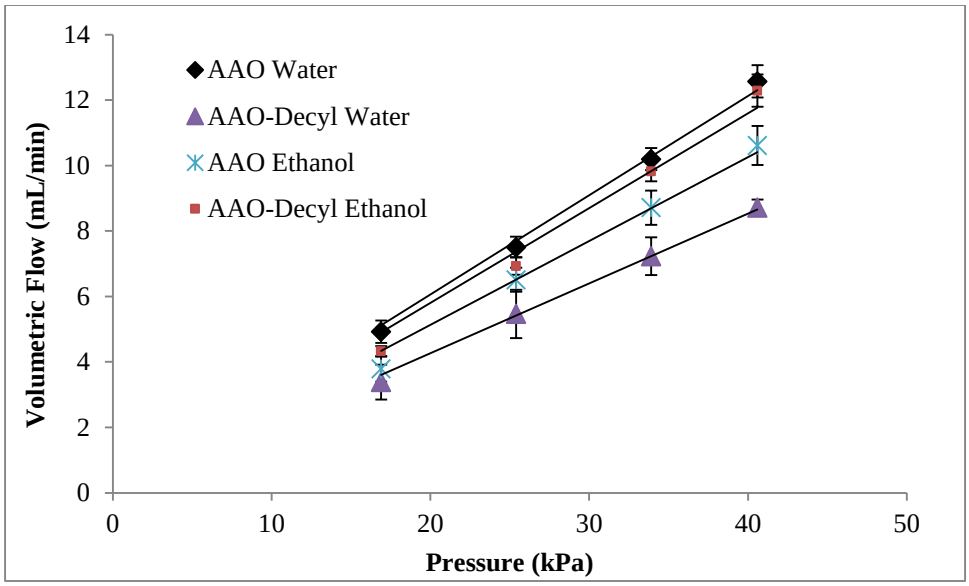

Figure 3.5. Flux of water and ethanol through AAO supports before and after exposure to the alkyl functionalization procedure of o-HCP thin film membranes. The same AAO membrane was used for all solvents.

The flux of ethanol and water before and after functionalization of the o-HCP membranes is presented in Figure 3.6. Ethanol flux was very similar before and after functionalization for each pressure suggesting that the decyl groups are not blocking the pores. The small error in each trial coupled with the FTIR results show that the decyl groups are not only present but also well adhered to the membrane surfaces. If the decyl groups were not bound to the surfaces of the membrane, it would be expected that the rapid flux through the membranes would wash the groups away. Instead, the flux is seen to remain stable with further trials potentially indicating that not only in the functional group tightly bound, but the membrane is selective to solvents.

In the presence of the hydrophilic solvent (water) the flux decreased dramatically after functionalization. The slope of the water flux as function of pressure drop for both

the o-HCP and AAO membranes decreased by 20% and 30%, respectively. This can be attributed to an effect by the hydrophobic functional group deterring the water from the pore spaces in the membrane. This suggests that a chemically selective separation can be achieved using the nanoporous membranes that have been functionalized.

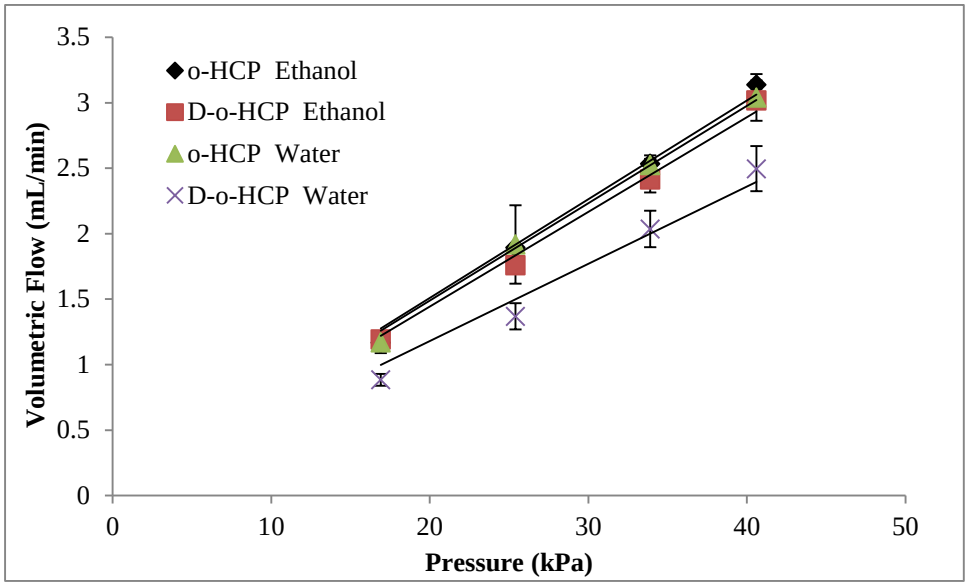

Figure 3.6. Flux of water and ethanol through o-HCP membranes before and after exposure to the alkyl functionalization procedure of o-HCP thin film membranes. The same o-HCP membrane was used for all solvents.

CONCLUSION

Functionalized silica thin films deposited onto macroporous supports can be used for a very selective separation. They have been shown to selectively allow permeation by different solvents while not limiting the flow of a neutral solvent demonstrating that the pores are not simply clogged. The use of contact angle also confirmed that the surface of the membrane is highly hydrophobic after functionalization. The presence of the decyl groups on the surface of the membranes was demonstrated with the use of FTIR by the presence of C-H stretching bands. Compared to the bare AAO support after functionalization, the o-HCP membrane displayed higher amounts of the alkyl group based on the FTIR results suggesting the D-o-HCP films contain more decyl than the functionalized bare AAO. The pressure-driven flux of water changed dramatically in both the AAO support and o-HCP membrane after exposure to the decyl functionalization procedure proving the properties of the membrane were drastically altered. However, the ethanol flux was relatively constant, suggesting that the membrane pores were not blocked during functionalization. Future studies with chemically altering the surface of the film would include measuring the extent of functionalization as well as using different functional groups to achieve different separations. The size exclusion characteristics of the o-HCP membranes coupled with the chemical selectivity of the functionalized films shows promise for applying this system to advanced separations.

Chapter Four: FUTURE WORK

The future directions for this project contain a number of paths due to the large range of applications of the project itself. This work successfully demonstrated that the synthesis of thin silica films with orthogonal pore orientation could be translated to thin film silica membranes with size and chemical selectivity. The functionalization of the membranes can be further optimized, solute diffusion and separation from the functionalized membranes can be examined. In addition whole cells can be separated with the functionalized films for purification or product accumulation. Finally, the separation properties of the membranes may be modeled.

Further experiments could follow on the demonstration of the interactions of the solvents and functionalized membranes. Specifically, diffusion studies with different molecules would further demonstrated chemical selectivity of the functionalized membranes and guide the optimization of the functionalization process. A more neutral solvent for the solutes, as compared to chapter two, is necessary so the solvent itself does not lead to interactions with the membrane, as suggested by chapter three, potentially skewing the results of diffusion. Hindered diffusion as described in chapter one can be compared to bulk diffusion. Mass accumulation in the pores should also be measured for the functionalized membrane for comparison of non-functionalized mass accumulation. Membrane transport models that include the partitioning of the solute between the solvent and the membrane surface, incorporated as a resistance in series, can be investigated. The functionalized surface may lead to less accumulation due to its selective nature.

Comparing permeability of the molecules to non-functionalized should also be completed to further characterize the functionalized membranes. Hydrophilic molecules of the same size as the hydrophobic should not diffuse as well. This observation would suggest chemical as well as size selectivity capabilities of the functionalized films.

Further imaging may be done as well to obtain more accurate images. SEM images were difficult to obtain because of the conductive surface of the AAO support covered by the nonconductive film of silica. The AAO support would charge the silica surface when bombarded with electrons creating a grainy image. Using an SEM with higher vacuum capable of a lower voltage may produce a better image. TEM images were difficult to obtain due to the thickness of the entire membrane system and difficulty in removing only the silica film. Further work in TEM imaging would be with further acid techniques to dissolve the AAO support but to deposit the sample in solution onto the carbon grid. This would involve using an acid that would not dissolve the carbon grid as well.

The potential applications of the thin film silica membranes that lead to future work are whole cell separations, and drug or natural product recovery. The small pores would make it possible to be used for cell purification as well as separate the cells from their products. Drug recovery could also be done by size and chemical selectivity of the membranes while recovering a significant amount by limiting mass accumulation in the pores. In conclusion, this work would eventually be applied to enhanced separation of small solutes, protein or cell purification, and even drug detection. The conversion of this system into a potentially larger size scale would be

appropriate based on the broad potential of metal oxide thin films as components of membranes. A current limitation of scaling up these membranes and configuring the membranes into more conventional geometries (hollow fiber membranes, for example) is their brittleness. However, the applicability of this thin film synthesis approach to a variety of membrane supports suggests that an improved match between thin film and support could be used to achieve improved mechanical stability of the films for larger scale applications.

REFERENCES

Alberius, P. C. A., Frindell, K. L., Hayward, R. C., Kramer, E. J., Stucky, G. D., & Chmelka, B. F. (2002). General predictive syntheses of cubic, hexagonal, and lamellar silica and titania mesostructured thin films. *Chemistry of Materials, 14*(8), 3284-3294. doi: 10.1021/cm011209u

Ansari, Shakeel Ahmed, & Husain, Qayyum. (2012). Potential applications of enzymes immobilized on/in nano materials: A review. *Biotechnology Advances, 30*(3), 512-523. doi: 10.1016/j.biotechadv.2011.09.005

Ariga, Katsuhiko, Vinu, Ajayan, Yamauchi, Yusuke, Ji, Qingmin, & Hill, Jonathan P. (2012). Nanoarchitectonics for Mesoporous Materials. *Bulletin of the Chemical Society of Japan, 85*(1), 1-32. doi: 10.1246/bcsj.20110162

Asuri, Prashanth, Bale, Shyam Sundhar, Pangule, Ravindra C., Shah, Dhiral A., Kane, Ravi S., & Dordick, Jonathan S. (2007). Structure, function, and stability of enzymes covalently attached to single-walled carbon nanotubes. *Langmuir, 23*(24), 12318-12321. doi: 10.1021/la702091c

Berlier, G., Gastaldi, L., Ugazio, E., Miletto, I., Iliade, P., & Sapino, S. (2013). Stabilization of quercetin flavonoid in MCM-41 mesoporous silica: positive effect of surface functionalization. *Journal of Colloid and Interface Science, 393,* 109-118. doi: 10.1016/j.jcis.2012.10.073

Boffa, V., ten Elshof, J. E., & Blank, D. H. A. (2007). Preparation of templated mesoporous silica membranes on macroporous alpha-alumina supports via direct coating of thixotropic polymeric sols. *Microporous and Mesoporous Materials, 100*(1-3), 173-182. doi: 10.1016/j.micromeso.2006.10.035

Brinker, C. J., Lu, Y. F., Sellinger, A., & Fan, H. Y. (1999). Evaporation-induced self-assembly: Nanostructures made easy. *Advanced Materials, 11*(7), 579-+. doi: 10.1002/(sici)1521-4095(199905)11:7<579::aid-adma579>3.0.co;2-r

Cang-Rong, Jason Teng, & Pastorin, Giorgia. (2009). The influence of carbon nanotubes on enzyme activity and structure: investigation of different immobilization procedures through enzyme kinetics and circular dichroism studies. *Nanotechnology, 20*(25). doi: 10.1088/0957-4484/20/25/255102

Chowdhury, S. R., Schmuhl, R., Keizer, K., ten Elshof, J. E., & Blank, D. H. A. (2003). Pore size and surface chemistry effects on the transport of hydrophobic and hydrophilic solvents through mesoporous gamma-alumina and silica MCM-48. *Journal of Membrane Science, 225*(1-2), 177-186. doi: 10.1016/j.memsci.2003.07.018

Coll, Carmen, Martinez-Manez, Ramon, Marcos, M. Dolores, Sancenon, Felix, & Soto, Juan. (2007). A simple approach for the selective and sensitive colorimetric

detection of anionic surfactants in water. *Angewandte Chemie-International Edition, 46*(10), 1675-1678. doi: 10.1002/anie.200603800

Collinson, M. M. (1999). Sol-gel strategies for the preparation of selective materials for chemical analysis. *Critical Reviews in Analytical Chemistry, 29*(4), 289-311. doi: 10.1080/10408349891199310

Cussler, E.L. (2009). *Diffusion: Mass Transfer in Fluid Systems* (Third ed.). 2009: Cambridge University Press.

Darvishmanesh, Siavash, Buekenhoudt, Anita, Degreve, Jan, & Van der Bruggen, Bart. (2009). General model for prediction of solvent permeation through organic and inorganic solvent resistant nanofiltration membranes. *Journal of Membrane Science, 334*(1-2), 43-49. doi: 10.1016/j.memsci.2009.02.013

Darvishmanesh, Siavash, Degreve, Jan, & Van der Bruggen, Bart. (2009). Comparison of pressure driven transport of ethanol/n-hexane mixtures through dense and microporous membranes. *Chemical Engineering Science, 64*(17), 3914-3927. doi: 10.1016/j.ces.2009.05.032

Das, Saikat, Wu, Qingliu, Garlapalli, Ravinder K., Nagpure, Suraj, Strzalka, Joseph, Jiang, Zhang, & Rankin, Stephen E. (2014). In-Situ GISAXS Investigation of Pore Orientation Effects on the Thermal Transformation Mechanism in Mesoporous Titania Thin Films. *The Journal of Physical Chemistry C, 118*(2), 968-976. doi: 10.1021/jp406165v

Davis, M. E. (2002). Ordered porous materials for emerging applications. *Nature, 417*(6891), 813-821. doi: 10.1038/nature00785

Deen, W. M. (1987). HINDERED TRANSPORT OF LARGE MOLECULES IN LIQUID-FILLED PORES. *Aiche Journal, 33*(9), 1409-1425. doi: 10.1002/aic.690330902

Dullien, F. A. L., & Shemilt, L. W. (1960). EQUATIONS FOR DETERMINING DIFFUSION COEFFICIENTS IN LIQUID SYSTEMS BY THE DIAPHRAGM CELL TECHNIQUE. *Nature, 187*(4739), 767-768. doi: 10.1038/187767a0

Edler, K. J., Goldar, A., Hughes, A. V., Roser, S. J., & Mann, S. (2001). Structural studies on surfactant-templated silica films grown at the air/water interface. *Microporous and Mesoporous Materials, 44*, 661-670. doi: 10.1016/s1387-1811(01)00247-5

Edler, K. J., & Roser, S. J. (2001). Growth and characterization of mesoporous silica films. *International Reviews in Physical Chemistry, 20*(3), 387-466.

Fan, H. Y., Hartshorn, C., Buchheit, T., Tallant, D., Assink, R., Simpson, R., . . . Brinker, C. J. (2007). Modulus-density scaling behaviour and framework architecture of

nanoporous self-assembled silicas. *Nature Materials, 6*(6), 418-423. doi: 10.1038/nmat1913

Feng, L., Li, S. H., Li, Y. S., Li, H. J., Zhang, L. J., Zhai, J., . . . Zhu, D. B. (2002). Super-hydrophobic surfaces: From natural to artificial. *Advanced Materials, 14*(24), 1857-1860. doi: 10.1002/adma.200290020

Fujii, T., Yano, T., Nakamura, K., & Miyawaki, O. (2001). The sol-gel preparation and characterization of nanoporous silica membrane with controlled pore size. *Journal of Membrane Science, 187*(1-2), 171-180. doi: 10.1016/s0376-7388(01)00338-6

Fujita, S., Koiwai, A., Kawasumi, M., & Inagaki, S. (2013). Enhancement of Proton Transport by High Densification of Sulfonic Acid Groups in Highly Ordered Mesoporous Silica. *Chemistry of Materials, 25*(9), 1584-1591. doi: 10.1021/cm303950u

Goux, A., Etienne, M., Aubert, E., Lecomte, C., Ghanbaja, J., & Walcarius, A. (2009). Oriented Mesoporous Silica Films Obtained by Electro-Assisted Self-Assembly (EASA). *Chemistry of Materials, 21*(4), 731-741. doi: 10.1021/cm8029664

Guliants, V. V., Carreon, M. A., & Lin, Y. S. (2004). Ordered mesoporous and macroporous inorganic films and membranes. *Journal of Membrane Science, 235*(1-2), 53-72. doi: 10.1016/j.memsci.2004.01.019

Hench, L. L., & West, J. K. (1990). THE SOL-GEL PROCESS. *Chemical Reviews, 90*(1), 33-72. doi: 10.1021/cr00099a003

Hosoya, O., Chono, S., Saso, Y., Juni, K., Morimoto, K., & Seki, T. (2004). Determination of diffusion coefficients of peptides and prediction of permeability through a porous membrane. *Journal of Pharmacy and Pharmacology, 56*(12), 1501-1507. doi: 10.1211/0022357044878

Jiang, F. J., Li, H. B., Di, Z. G., Sui, S., Yu, Q. C., & Zhang, J. L. (2013). Silica ultrafiltration membrane with tunable pore size for macromolecule separation. *Journal of Membrane Science, 441*, 25-30. doi: 10.1016/j.memsci.2013.04.008

Johnston, T. P., Salamat-Miller, N. T., Alur, H. H., & Mitra, A. K. (2003). An attempt to modulate the microporous diffusion of a model polypeptide by altering its secondary structure. *Drug Delivery, 10*(2), 65-72. doi: 10.1080/10717540390169610

Koganti, V. R., Dunphy, D., Gowrishankar, V., McGehee, M. D., Li, X. F., Wang, J., & Rankin, S. E. (2006). Generalized coating route to silica and titania films with orthogonally tilted cylindrical nanopore arrays. *Nano Letters, 6*(11), 2567-2570. doi: 10.1021/nl061992v

Konganti, Venkat. (2006). *Synthesis and Transport Properties of Oriented, Accessible Hexagonal Mesoporous Silica Nanofiltration Membranes on Macroporous*

Supports. (PhD in Chemical Engineering), University of Kentucky, Lexington, Kentucky.

Lu, Y. F., Ganguli, R., Drewien, C. A., Anderson, M. T., Brinker, C. J., Gong, W. L., . . . Zink, J. I. (1997). Continuous formation of supported cubic and hexagonal mesoporous films by sol gel dip-coating. *Nature, 389*(6649), 364-368.

Machado, D. R., Hasson, D., & Semiat, R. (2000). Effect of solvent properties on permeate flow through nanofiltration membranes - Part II. Transport model. *Journal of Membrane Science, 166*(1), 63-69. doi: 10.1016/s0376-7388(99)00251-3

Maeda, K., Ichinose, K., Yamazaki, T., & Suzuki, T. (2008). Preparation of mesostructured silica/anodic alumina composite membranes in mild conditions using acetic acid. *Microporous and Mesoporous Materials, 112*(1-3), 603-611. doi: 10.1016/j.micromeso.2007.10.043

Majumder, M., Chopra, N., & Hinds, B. J. (2011). Mass Transport through Carbon Nanotube Membranes in Three Different Regimes: Ionic Diffusion and Gas and Liquid Flow. *Acs Nano, 5*(5), 3867-3877. doi: 10.1021/nn200222g

Markovics, Akos, & Kovacs, Barna. (2013). Fabrication of optical chemical ammonia sensors using anodized alumina supports and sol-gel method. *Talanta, 109*, 101-106. doi: 10.1016/j.talanta.2013.01.054

McCool, B. A., Hill, N., DiCarlo, J., & DeSisto, W. J. (2003). Synthesis and characterization of mesoporous silica membranes via dip-coating and hydrothermal deposition techniques. *Journal of Membrane Science, 218*(1-2), 55-67. doi: 10.1016/s0376-7388(03)00136-4

Membrane Handbook. (2001). (W. S. W. Ho & K. K. Sirkar Eds.). Norwell, Massachusetts: Kluwer Academic Publishers.

Nazeeruddin, M. K., Di Censo, D., Humphry-Baker, R., & Gratzel, M. (2006). Highly selective and reversible optical, colorimetric, and electrochemical detection of mercury(II) by amphiphilic ruthenium complexes anchored onto mesoporous oxide films. *Advanced Functional Materials, 16*(2), 189-194. doi: 10.1002/adfm.200500309

Nishiyama, N., Park, D. H., Koide, A., Egashira, Y., & Ueyama, K. (2001). A mesoporous silica (MCM-48) membrane: preparation and characterization. *Journal of Membrane Science, 182*(1-2), 235-244. doi: 10.1016/s0376-7388(00)00570-6

Palaniappan, Al, Li, Xu, Tay, Francis E. H., Li, Jun, & Su, Xiaodi. (2006). Cyclodextrin functionalized mesoporous silica films on quartz crystal microbalance for enhanced gas sensing. *Sensors and Actuators B-Chemical, 119*(1), 220-226. doi: 10.1016/j.snb.2005.12.015

Park, D. H., Nishiyama, N., Egashira, Y., & Ueyama, K. (2001). Enhancement of hydrothermal stability and hydrophobicity of a silica MCM-48 membrane by silylation. *Industrial & Engineering Chemistry Research, 40*(26), 6105-6110. doi: 10.1021/ie0103761

Park, D. H., Nishiyama, N., Egashira, Y., & Ueyama, K. (2003). Separation of organic/water mixtures with silylated MCM-48 silica membranes. *Microporous and Mesoporous Materials, 66*(1), 69-76. doi: 10.1016/j.micromeso.2003.08.025

Peterson, G. L. (1977). SIMPLIFICATION OF PROTEIN ASSAY METHOD OF LOWRY ET AL - WHICH IS MORE GENERALLY APPLICABLE. *Analytical Biochemistry, 83*(2), 346-356. doi: 10.1016/0003-2697(77)90043-4

Platschek, B., Keilbach, A., & Bein, T. (2011). Mesoporous Structures Confined in Anodic Alumina Membranes. *Advanced Materials, 23*(21), 2395-2412. doi: 10.1002/adma.201002828

Platschek, B., Petkov, N., & Bein, T. (2006). Tuning the structure and orientation of hexagonally ordered mesoporous channels in anodic alumina membrane hosts: A 2D small-angle X-ray scattering study. *Angewandte Chemie-International Edition, 45*(7), 1134-1138. doi: 10.1002/anie.200503301

Postel, Stefanie, Spalding, Gerd, Chirnside, Morfula, & Wessling, Matthias. (2013). On negative retentions in organic solvent nanofiltration. *Journal of Membrane Science, 447*(0), 57-65. doi: http://dx.doi.org/10.1016/j.memsci.2013.06.009

Robinson, J. P., Tarleton, E. S., Millington, C. R., & Nijmeijer, A. (2004). Solvent flux through dense polymeric nanofiltration membranes. *Journal of Membrane Science, 230*(1-2), 29-37. doi: 10.1016/j.memsci.2003.10.027

Ruiz-Hitzky, Eduardo, Darder, Margarita, Aranda, Pilar, & Ariga, Katsuhiko. (2010). Advances in Biomimetic and Nanostructured Biohybrid Materials. *Advanced Materials, 22*(3), 323-336. doi: 10.1002/adma.200901134

Velev, O. D., Jede, T. A., Lobo, R. F., & Lenhoff, A. M. (1997). Porous silica via colloidal crystallization. *Nature, 389*(6650), 447-448. doi: 10.1038/38921

Velev, O. D., Jede, T. A., Lobo, R. F., & Lenhoff, A. M. (1998). Microstructured porous silica obtained via colloidal crystal templates. *Chemistry of Materials, 10*(11), 3597-3602. doi: 10.1021/cm980444i

Velleman, L., Triani, G., Evans, P. J., Shapter, J. G., & Losic, D. (2009). Structural and chemical modification of porous alumina membranes. *Microporous and Mesoporous Materials, 126*(1-2), 87-94. doi: 10.1016/j.micromeso.2009.05.024

Vinu, A., Hossain, K. Z., & Ariga, K. (2005). Recent advances in functionalization of mesoporous silica. *Journal of Nanoscience and Nanotechnology, 5*(3), 347-371. doi: 10.1166/jnn.2005.089

Yoshitake, H. (2005). Highly-controlled synthesis of organic layers on mesoporous silica: their structure and application to toxic ion adsorptions. *New Journal of Chemistry, 29*(9), 1107-1117. doi: 10.1039/b504957a

Zha, Jianing, & Roggendorf, Hans. (1991). Sol–gel science, the physics and chemistry of sol–gel processing, Ed. by C. J. Brinker and G. W. Scherer, Academic Press, Boston 1990, xiv, 908 pp., bound—ISBN 0-12-134970-5. *Advanced Materials, 3*(10), 522-522. doi: 10.1002/adma.19910031025

Zhang, J. L., Li, W., Meng, X. K., Wang, L., & Zhu, L. (2003). Synthesis of mesoporous silica membranes oriented by self-assembles of surfactants. *Journal of Membrane Science, 222*(1-2), 219-224. doi: 10.1016/s0376-7388(03)00292-8

Zhao, D. Y., Feng, J. L., Huo, Q. S., Melosh, N., Fredrickson, G. H., Chmelka, B. F., & Stucky, G. D. (1998). Triblock copolymer syntheses of mesoporous silica with periodic 50 to 300 angstrom pores. *Science, 279*(5350), 548-552. doi: 10.1126/science.279.5350.548

Zhao, D. Y., Huo, Q. S., Feng, J. L., Chmelka, B. F., & Stucky, G. D. (1998). Nonionic triblock and star diblock copolymer and oligomeric surfactant syntheses of highly ordered, hydrothermally stable, mesoporous silica structures. *Journal of the American Chemical Society, 120*(24), 6024-6036. doi: 10.1021/ja974025i

Zhao, D., Yang, P., Melosh, N., Feng, J., Chmelka, B. F., & Stucky, G. D. (1998). Continuous mesoporous silica films with highly ordered large pore structures. *Advanced Materials, 10*(16), 1380-+. doi: 10.1002/(sici)1521-4095(199811)10:16<1380::aid-adma1380>3.0.co;2-8

VITA

Mary Kaitlyn Clark Wooten

EDUCATION

Bachelors of Science in Chemical Engineering, Minor in Mathematics, Cum Laude, University of Kentucky, May 2012

EXPERIENCE

Graduate Research Assistant, Department of Chemical and Materials Engineering, University of Kentucky, August 2012- December 2014, Advisor, Dr. Barbara Knutson

IGERT (Integrated Graduate Education and Research Traineeship), Bioactive interfaces and devices, Department of Chemical and Materials Engineering, University of Kentucky, August 2012- August 2013, Advisors, Dr. Barbara Knutson and Dr. Stephen Rankin

Undergraduate Research Lab Assistant, Department of Chemical and Materials Engineering, University of Kentucky, Research Experience for Undergraduates (REU) from National Science Foundation (NSF), May 2011- May 2012, Supervisor, Dr. Barbara Knutson

TECHNICAL PRESENTATIONS

Clark, M., B. Knutson, S. Rankin. 2011. Synthesis of Thin Film Silica Membranes for the Recovery of Proteins. American Institute of Chemical Engineers: National Conference October 2011, Minneapolis, Minnesota

Clark, M., B. Knutson, S. Rankin. 2012. Synthesis of Thin Film Silica Membranes for the Recovery of Proteins. American Institute of Chemical Engineers: Regional Conference April 2012, Clemson University, South Carolina.

Wooten, M., B. Knutson, S. Rankin. 2013. Nanofiltration Membranes from Oriented Mesoporous Silica Thin Films. Kentucky Nano-Symposium August 2013, University of Louisville, Kentucky.